Title
Mass Transfer Phenomena and Pharmacokinetics in Topical Delivery of anti-HIV Microbicides

Author
Funke, Claire

Publication Date
2018

Peer reviewed|Thesis/dissertation

Mass Transfer Phenomena and Pharmacokinetics in Topical Delivery of anti-HIV Microbicides

by

Claire Funke

A dissertation submitted in partial satisfaction of the

requirements for the degree of

Doctor of Philosophy

in

Engineering - Mechanical Engineering

in the

Graduate Division

of the

University of California, Berkeley

Committee in charge:

Professor Andrew J. Szeri, Chair
Professor Maria Ekstrand
Professor Mohammad R.K. Mofrad

Summer 2018

Mass Transfer Phenomena and Pharmacokinetics in Topical Delivery of anti-HIV Microbicides

Abstract

Mass Transfer Phenomena and Pharmacokinetics in Topical Delivery of anti-HIV Microbicides

by

Claire Funke

Doctor of Philosophy in Engineering - Mechanical Engineering

University of California, Berkeley

Professor Andrew J. Szeri, Chair

Topically applied anti-HIV microbicides are placed within a cultural, economic, and ethical context in order to motivate research into their development. This leads to the creation of a multi-scale, multi-step numerical model that incorporates gel spreading and drug diffusion. Use of this model allows conclusions to be drawn about how rheological characteristics of non-Newtonian gels affects the ultimate amount of drug being delivered into tissue. Dilution of the gels by natural fluid production has a strong effect on drug delivery, and osmolarity is investigated as a potential driver of fluid flow into (or out of) the lumen. The equations governing osmolarity driven solvent flow yield two dimensionless groups that can be optimized to produce improved drug delivery. Finally, osmolarity driven fluid flux is incorporated into the numerical model of gel spreading and drug diffusion, and an engineered gel is proposed.

I dedicate this dissertation to Ashwin, my parents, my labmates, and everyone who has supported me through this entire process. I would have been lost without your continuous stream of love and encouragement.

Contents

List of Figures

List of Tables

Acknowledgments

The majority of Chapter 2: Gels was published previously in the journal Chemical Engineering Science with the title: Coupled gel spreading and diffusive transport models describing microbicidal drug delivery.

I would also like to acknowledge the Department of Mechanical Engineering as well as the Graduate Division which both generously provided research stipends to support me while completing this research.

Chapter 1

Introduction

1.1 HIV

Human Immunodeficiency Virus (HIV) is the virus that leads to Acquired Immunodeficiency Syndrome (AIDS). The syndrome was first reported in the United States in 1981, and two years later, the virus itself was isolated. By tracing the epidemic back to its origins, Faria et al. [25] found that the globally predominant kind of HIV (type 1 group M) has its roots in early 1920s Kinshasa in the Democratic Republic of the Congo. Around this time, the corresponding simian immunodeficiency virus (SIV) was first transmitted to a human (likely within the context of bushmeat hunting [69]). The spread of the virus was limited until the 1950s when the use of dirty needles for immunizations combined with an increased number of customers per sex worker in Kinshasa led to an exponential growth of the infection rate [25]. Around 1966, the virus made its way to Haiti from which it eventually spread to the United States and gained widespread attention for its devastating effects on the gay population of San Francisco [32].

The virus was first isolated in 1983 by doctors at the Pasteur Institute in France who called the retrovirus Lymphadenopathy-Associated Virus (LAV) [6]. In the United States, researchers at the National Cancer Institute determined that AIDS was caused by a member of the human T-cell leukemia virus family designated HTLV-III in 1984 [50]. It was shortly thereafter that the two were determined to be the same virus (HIV), and a commercial blood test, ELISA, was licensed to screen for it [63]. At the time, it was hoped that a vaccine could be developed within two years, a goal which to this day has yet to be achieved.

The desperate drive to understand HIV/ AIDS and halt the burgeoning epidemic led to relatively rapid progress, particularly in the western world. In terms of treatment, Zidovudine (AZT) was approved by the FDA as treatment for HIV in 1987, a mere four years after the virus was recognized [58]. The drug is a nucleoside reverse transcriptase inhibitor meaning that it interferes with the enzyme that HIV uses to make DNA thereby decreasing replication of the virus. At this point in time, the major known routes of transmission were sexual contact, IV drug use, blood transfusions, and from mother to child. Casual contact had

already been ruled out as a transmission risk, though fear of contracting the disease built a large social stigma against interacting with people diagnosed with HIV [14].

By 1995, Saquinivir was approved by the FDA to be used in combination with AZT ushering in a new era of highly active anti retroviral treatment (HAART). As a protease inhibitor, Saquinivir functions by blocking the action of an enzyme that allows newly formed virions to become infectious. Once incorporated into clinical practice, HAART brought the rate of AIDS related deaths and hospitalization down by 60% to 80% in the countries that could afford it [40].

Currently in the United States, around 1.2 million people are living with HIV of which an estimated one in eight is unaware of their status. Life expectancy for people living with HIV in the US has been increasing over the years as improved treatment therapies have been released, so the total number of people living with HIV has been increasing despite a relatively stable rate of new infections at around 50,000 per year. The disease is primarily spread in the population of men who have sex with men (MSM) in the US with black and Hispanic MSM at particular risk [12]. Individuals determined to be members of at-risk populations are eligible to be prescribed a daily oral pre-exposure prophylaxis (PrEP), approved by the FDA in 2012, to reduce their likelihood of infection [81].

1.2 Epidemic in sub-Saharan Africa

Globally, around 36.7 million people are living with HIV. Of those, 19.4 million (53%) live in sub-Saharan Africa, a region that is home to a mere 6.2% of the global population [80]. The severity of the HIV epidemic in the region is clearly evident in Figure (1.1) which shows adult HIV prevalence as of 2016 [28]. In many western countries, the epidemics are concentrated in specific high-risk subpopulations (general prevalence of less than 1% with a prevalence greater than 5% in subgroups), but the epidemic is generalized in much of sub-Saharan Africa with prevalences over 1% and reaching as high as 26% in Swaziland [80].

In addition to carrying a disproportionate burden in terms of general prevalence, sub-Saharan Africa accounts for over 70% of global new infections and around 74% of AIDS related deaths [42]. Women in particular are at risk accounting for 59% of the people living with HIV in the region [80]. When compared to the United States, where women account for only 19% of new HIV diagnoses, the difference is striking [38]. Focusing on preventing young women in sub-Saharan Africa from contracting HIV would have a large impact on the global HIV burden.

In contrast with the epidemic in the United States, heterosexual sex is the primary mode of transmission in sub-Saharan Africa [42]. A small portion of the gender disparity can therefore be attributed to the fact that women are physiologically more susceptible to HIV infection than men [62]. However the greater portion of the difference is due to social and cultural norms that put young women at risk. It is not uncommon for young women with a lack of financial security to engage in transactional relationships with older men in exchange for food, money, or shelter. In these relationships, and indeed in nearly any relationship, it

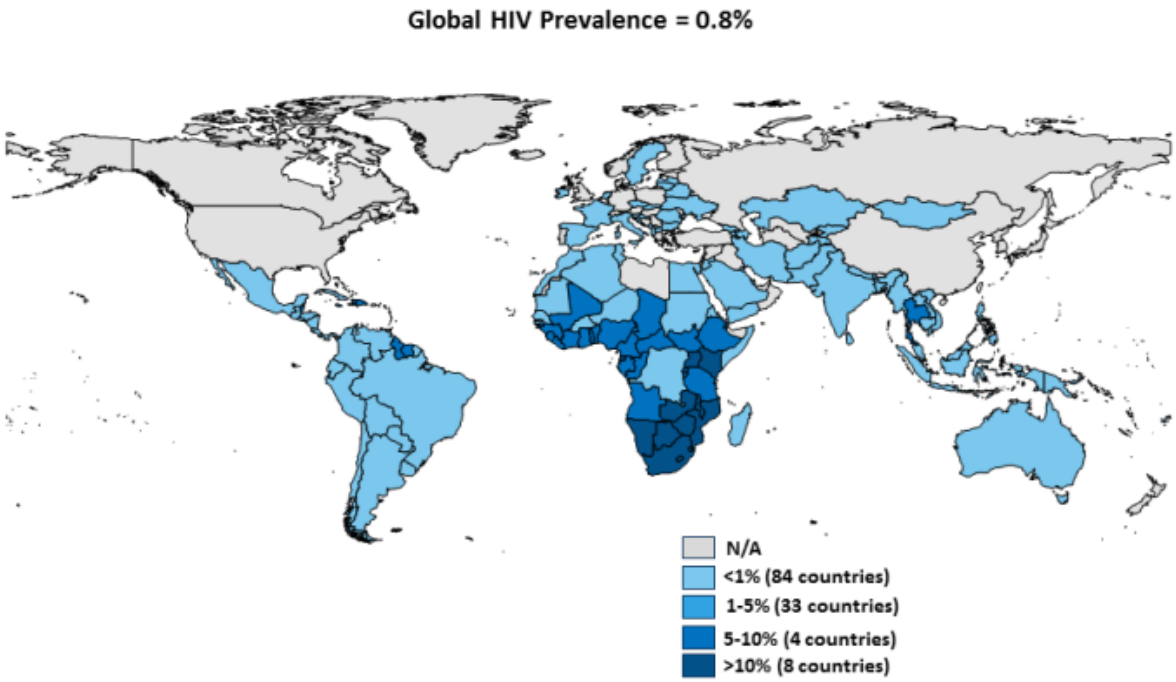

Figure 1.1: Adult HIV prevalence by country in 2016. This map was produced by the Kaiser Family Foundation, based on UNAIDS, AIDSinfo [28].

is difficult for women to negotiate safe sex behaviors because of financial dependency and the risk of domestic violence [71]. Even monogamous married women are at risk because of the pervasiveness of men having multiple sexual partners thereby exposing themselves and their wives to risk [9].

1.3 Interventions

Early prevention interventions in sub-Saharan Africa focused on a behavioral intervention called the ABC approach – Abstinence, Be faithful, use a Condom. These programs were strongly supported by the US President's Emergency Plan for AIDS Relief (PEPFAR), with abstinence until marriage being a particular focus of funding [66]. Though the ABC approach is still broadly in use, the focus on abstinence has fallen from favor as it fails to address women's social and economic vulnerabilities [36]. It also fails to account for more general underlying socio-cultural, economic, and political factors which has led to a current push toward combination prevention approaches that use complementary structural, behavioral, and biomedical prevention strategies to stem the spread of HIV. Although the majority of this thesis focuses on one specific biomedical intervention, a non-comprehensive overview of some of these prevention interventions are given here.

Structural

A structural intervention attempts to address social, economic, political, or environmental factors that make people vulnerable to HIV infection. As has already been pointed out in Section 1.2, one such factor is gender inequality and domestic violence putting young women at risk. Also at a disadvantage are sex workers who fear being arrested and imprisoned for their livelihoods which prevents them from accessing proper health care increasing their own risk as well as their clients'. Dealing with these issues involves high level types of interventions, the effects of which tend to be long term and difficult to measure [34].

For example, equalizing the social power dynamic between genders could both empower women to stand up for themselves in demanding safer sexual practices and encourage men to respect women as individuals with agency [34, 61, 79]. But breaking down a social structure as deeply embedded as sexism is no small task. Program H, designed and implemented in Brazil, encourages young men to look critically at gender norms and stereotypical gender roles. Self-reported behaviors and opinions of young men who have participated in the program have shown a decrease in partner violence and an increase in contraceptive use, both of which are associated with decreased risk of HIV transmission [61]. However, implementing such a program on a national level and measuring its effects would be a daunting task and could take more than a generation to come to fruition.

A political intervention to reduce the transmission of HIV would be to decriminalize same-sex relationships, cross-dressing, sex work, and injection drug use. These populations face severe social stigma which makes it difficult to get new laws passed to protect them from legal punishment. Fear of running afoul of such laws prevents these people from seeking health care or accessing other HIV prevention programs which drives high rates of infection in these groups [7, 33, 80]. Portugal decriminalized drug possession for personal use and drug use itself in 2001. Although the rates of drug use have remained roughly the same, the negative outcomes of drug use (including HIV infection from injection drug use) have declined steadily since then [33]. Thus decriminalization of behaviors associated with elevated HIV risk has been shown to improve outcome, but the social stigma associated with such behaviors must also be addressed in order to enact such laws.

Behavioral

Behavioral interventions aim to reduce risky behaviors or incentivize safe behaviors in general or specific populations. This is the most commonly used type of intervention, and many have shown great promise in preventing HIV transmission. The ABC approach which has already been mentioned is the most widely known behavioral intervention for a general population. Another equally general intervention is educational efforts to combat stigma against people living with HIV. More targeted behavioral interventions might be aimed at young women to stay in school and to delay sexual debut.

Although it has long been known that casual contact cannot transmit HIV, survey responses have shown that concerns still exist in the general population that, for example,

an asymptomatic HIV positive teacher could infect one of her students during day to day events. Surveys have also shown a distinct "social distancing" from people living with HIV associated with stigma toward the disease [15]. In order to avoid these experiences, many refrain from getting tested or choose not to disclose their status to their partners in the event of a positive diagnosis which allows the spread of the virus to remain unimpeded. Education about the disease has been shown to be effective to reduce stigma experienced by people living with HIV [20]. Hence, large scale education interventions have been launched to combat misinformation, but results been mixed due to logistical challenges [84]. However, small scale studies have shown more consistent positive outcomes [11].

A more targeted intervention that has shown measurable positive results is cash transfers to poor women. The idea behind such transfers is to discourage risky sexual behaviors by closing the economic gap experienced by young women. Women who have enough money to afford basic necessities are more likely to stay in school, delay sexual debut, and engage in safer sex behaviors. Some studies have made the cash transfers conditional on school attendance or negative sexually transmitted infection (STI) tests while others have been unconditional cash transfers [4, 21, 73]. Data from these studies suggest that the intervention can be effective with or without conditions imposed on participants. However, scalability and cost make widespread implementation of such programs difficult to achieve [59].

Biomedical

Biomedical interventions are clinical or medicinal methods of reducing HIV transmission on an individual level. Used in conjunction with behavioral interventions, biomedical interventions can drastically reduce an person's risk of contracting HIV. The most common biomedical intervention is the use of barrier prophylactics (male or female condoms) which is a staple in the ABC approach. It has been estimated that around 45 million HIV infections have been averted through the use of condoms in the past 25 years [80].

Voluntary medical male circumcision (VMMC) is a surgical intervention that has been shown to reduce a man's risk of contracting HIV through vaginal insertive sex by up to 60%. The simple, outpatient procedure provides a level of protection similar to what would be achieved should a vaccine one day be produced [3]. Risk compensation behaviors (when an individual engages in riskier behaviors as a result of feeling safer due to an intervention) were not reported in regions with scaled up VMMC campaigns where safe sex counseling was provided at the time of procedure implying that there were distinct benefits conferred to participants [70].

Administering an anti-retroviral drug to HIV negative people who anticipate exposure to the virus, also known as PrEP (Pre-exposure prophylaxis), is another promising biomedical intervention. In the United States, PrEP is administered orally in the form of a prescription-only daily pill called Truvada that was licensed by Gilead Sciences in 2012 [39]. When used as directed, the pill can reduce a patient's risk of HIV infection by 70% [27]. However, at a cost of nearly $1300 per month per patient, it is not a viable option for widespread use in resource lacking regions [18].

Another very interesting biomedical intervention to prevent the transmission of HIV is treatment for HIV positive individuals. The idea behind Treatment as Prevention (TasP) is that when the viral load of an HIV positive individual is suppressed by antiretroviral drugs, the chances that they will infect someone else drop dramatically. The high effectiveness of TasP was demonstrated by the HIV Prevention Trial Network's trial 052 [17]. TasP is an attractive approach as it yields both personal benefits to the infected person in treatment as well as the public health benefit of reduced transmission rates. Again, cost is a limiting factor of scaling up such an intervention. It is also important to note that viral suppression (required for the effectiveness of TasP) is highly dependent on strict adherence to the treatment regimen which can be difficult to achieve [64].

1.4 Ethics of Intervention Research

Before any interventions are adopted on a large scale, they need to be studied in a small scale, controlled environment. This kind of research prevents large sums of money from being wasted on ineffective interventions and ensures that highly effective interventions can be adopted as quickly as possible. Although necessary, these kinds of studies come with distinct ethical challenges, particularly when they are performed in regions suffering from an economic disadvantage such as many parts of sub-Saharan Africa. Understanding the ethics of anti-HIV microbicide research is necessary to contextualize the work being done as well as to ensure that the recommendations made adhere to the best interests of the targeted demographics.

Generally speaking, the gold standard in clinical evaluation is the randomized control trial. In these trials, participants are randomly assigned to a control group or an intervention group. If the study is double blind, then neither the clinicians nor the participants know to which group an individual is assigned [54]. Within the context of microbicidal gel PrEP development, this would mean that the control group receives a placebo gel while the intervention group receives a gel loaded with an anti-HIV drug. The use of a placebo is defensible in this case as there is no current evidence that the intervention gel provides definite protective benefits. Both groups receive the same instructions for use [41, 51]. The use of control groups allows researchers to show that an intervention is effective based on differences between the two groups, the difference in this case being the rate at which participants contract HIV. The ethical challenge is readily apparent as researchers want positive results, but positive results require that a statistically significant number of study participants become infected with HIV.

There are several ways to address this conflict of interest, and the paramount concept to keep in mind is to do no harm and safeguard the wellbeing of the subjects as described in the Declaration of Helsinki by the World Medical Association [85]. At the very least, study participants should be no worse off than they were before the study began, though preferably all participants should stand to gain something from participation. Many studies begin by giving all participants educational seminars to encourage everyone to engage in

best practice preventive behavior such as using condoms, and often an unlimited supply condoms are provided for participants to take home [51]. The seminars must also reinforce that the biomedical intervention (in this case a microbicidal or placebo gel) *may or may not* work to prevent HIV infection in order to avoid risk compensation behaviors [82]. Providing educational seminars and condoms is a bare minimum procedure though as it reinforces that any positive results are due to the biomedical intervention as opposed to any (cheaper) behavioral changes.

In the best case scenario that the biomedical intervention is shown to have good results (i.e. significantly more control participants are infected with HIV), researchers need to plan ahead of time what to do for those who became infected during the trial as well as whether or not the intervention will continue to be supplied to the remaining participants who are uninfected. Assuming funding is not an issue, it would be socially responsible to provide HAART to those who became infected, particularly if it can be shown that participation in the study was linked with risk compensation behavior. As for the remaining participants, they would benefit from provision of the biomedical intervention, so ideally they would receive it post-study as a benefit of participation, at least for some limited amount of time.

This is particularly relevant in studies of interventions that are performed in poverty stricken nations but are intended for use in wealthy nations. There are many reasons to perform studies in poorer countries such as those in sub-Saharan Africa. The most clinically relevant of which is that the higher HIV incidence rates allow for a smaller study cohort and will show larger results in the event of an effective intervention. This in combination with the fact that conducting trials is cheaper and easier to pass legal challenges leads to many studies being conducted there. However, it is easy to slip into exploitative methods if researchers are not careful [1].

In the worst case scenario, a study must be halted either due to a lack of efficacy as was the case for the VOICE trial [53] or due to a large number of adverse event associated with the intervention arm of a trial (e.g. the use of lime juice douches at greater than 50% concentrations [37]). Halting a trial in these cases is an ethical necessity as the continuation would unnecessarily place participants at risk. In the case of adverse events, researchers have a responsibility to provide best available treatment [85].

Chapter 2

Gels

A more cost effective option for PrEP is a vaginally applied microbicide used pre- and/ or post-coitally. Women would be able to apply the gel privately using the device shown in Figure (2.1), and there would be no need to inform their partners thereby bypassing the social stigma attached to the use of barrier methods, or the implicit questions about a partner's infection status. Two of the drugs that are currently under investigation for use in microbicidal gels are Raltegravir and Tenofovir. Raltegravir is an integrase strand transfer inhibitor meaning that it interrupts the integration of viral DNA into host cell DNA. Because this step occurs rather late in the infection process, Raltegravir is well suited for post-coital application. A proof-of-concept study with macaques seems promising [22], but clinical knowledge of how the drug interacts with the human body is still lacking. Tenofovir, like Zidovudine, is a nucleotide reverse transcriptase inhibitor meaning that it prematurely terminates the replicated DNA strand thus ceasing viral replication. In order to be effective, Tenofovir must be applied prior to sex in order that it can be transformed into its bioactive form, Tenofovir diphosphate, and prevent the early stages of infection. Two trials using 4 mL of a hydroxyethylcellulose gel loaded with 1 percent concentration Tenofovir applied vaginally have had mixed results [74]. The CAPRISA 004 trial found a reduced transmission rate of approximately 39 percent [41], but the VOICE trial was discontinued prematurely as no demonstrable effect was found [53]. Though adherence to the dosage regimen appears to play some role in the discrepancy, no clear explanation exists to explain the differences in the trial outcomes. This is due in part to incomplete knowledge of the pharmacodynamics of vaginal drug delivery of microbicides.

In order to design an effective drug delivery system, one must have a thorough knowledge of the physics of the problem and the relative impacts of various design factors. Though it is possible to attain this knowledge through experimental studies alone, it is extremely costly in terms of both time and money which could lead to a premature abandonment of a promising system. It is therefore desirable to develop a computational model which can easily explore the various factors which may impact the effectiveness of they system. When supplemented with experimental data (e.g. gel rheological parameters or diffusion constants of a drug through various media), these computational models can be used to

Figure 2.1: Gel applicator used by the Microbicide Trial Network, University of Pittsburgh and Magee-Womens Research Institute [52].

uncover interesting physical phenomena that may otherwise have been left undiscovered and lend great insight into the problem itself.

Using available knowledge, several computational models have been developed in order to explore the drug delivery problem. Early on, the gel flow and drug transport problems were considered separately. Initial gel flow models approximated the vaginal walls as rigid and parallel [44, 43]. Later, flexible walls and a Reynolds lubrication approximation were used [75, 76]. In addition, boundary flux dilution (naturally produced fluid entering the lumen through the epithelium) was incorporated as a mass source term once an assumption of lateral gel fraction homogeneity was justified. A Carreau-like constitutive equation fitted to experimental data was used to model the shear-thinning gel with dilution as a constitutive parameter [76]. To address the drug transport part of the problem, Gao and Katz [31] simplified the geometry into a one dimensional multi-compartmental problem with the vaginal canal as a homogeneous source of drug. Their model had reasonable agreement with *in vivo* human studies. Looking at the problem within the vaginal canal, Tasoglu et al. [78]

extended their work by adding a two dimensional convection-diffusion equation with drug absorption at the walls. MacMillan [48] combined various concepts developed previously to formulate a model that concurrently solves for the gel motion and drug transport problems.

Something that was not previously analyzed is exactly how the properties of the fluid affect the delivery of drug to tissue. There are several gels which can be considered as candidates for use in this application, and their individual properties can have significant effects on the final results. The rheological sensitivity of a gel to dilution, for example, may determine whether or not diluting flux from the wall boundaries needs to be taken into consideration. Therefore, as a companion study to MacMillan's, the aim of this chapter and also the associated paper (Funke et al. [29]) is to investigate how modifying gel rheological parameters affects flow and drug transport and to compare the behavior of three different gels under varying sets of simulated conditions. In addition, the importance of gel coverage and concentration gradient to the delivery of the drug (in this case Tenofovir) to the tissue is discussed. Finally, conclusions are drawn about how modifying gel rheological parameters affects the rate of delivery of the microbicide to the tissue.

2.1 Modelling Mass Transport

After placing the gel bolus into the vaginal canal, typically using a piston type applicator, the drug-loaded gel spreads along the vaginal wall into a thin layer. The spreading process is largely driven by squeezing from the muscular walls and takes place over the course of several hours. At the same time, the drug will diffuse from the gel into the mucosal tissue which is composed of two layers: the epithelium and the stroma. The drug, in this case tenofovir, first encounters vasculature in the stroma which is about 10% blood vessels by volume. Once the tenofovir molecules enter the blood stream, they are cleared from the region by the circulatory system. When tenofovir (TFV) enters a cell, it is converted into tenofovir diphosphate (TFV-DP) which is the bioactive form of tenofivir that acts as a reverse transcriptase inhibitor, preventing a critical early step of the infectious process [31]. Though critical to the goal of preventing infection, the rate at which TFV is converted into TFV-DP is quite slow, and loss of TFV due to conversion can be neglected in this model. In addition, human pharmacokinetic studies have shown that the concentrations of TFV and TFV-DP in the vaginal mucosal layer are proportional [68]. It is therefore pharmacologically meaningful to focus on TFV alone. The transport of TFV into the stromal tissue is driven by two coupled processes, the spreading of the gel and diffusive transport across concentration gradients. As the spreading is independent of the diffusion and occurs on a faster time scale, its numerical solution is used as an input to the numerical method of the diffusion process. The outputs that are of greatest interest are the distance spread by the gel along the canal over time and the measures of drug concentration over time in the gel, epithelial, and stromal compartment.

In order to derive the equations of motion governing gel spreading, a Reynolds lubrication approximation is applied to conservation statements of applied gel mass as well as total fluid

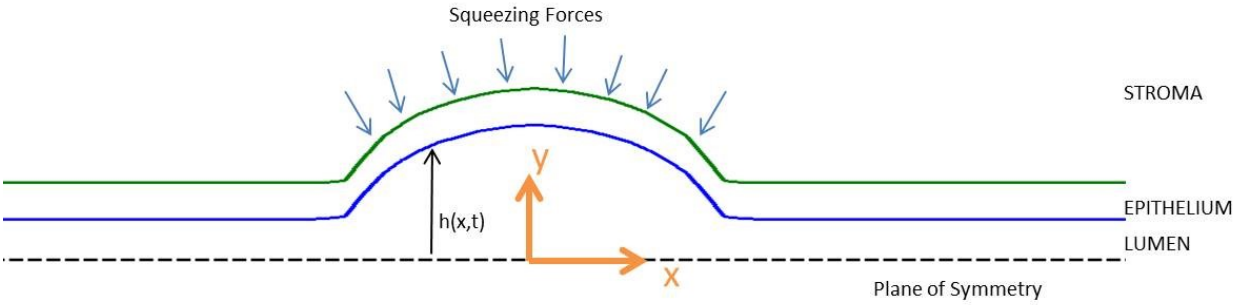

Figure 2.2: Definition sketch of the vaginal wall and surrounding tissue. Drawing not to scale.

mass (gel plus diluting fluid) [78]. In other words, because of the long and shallow cross-section of the vaginal canal, we argue that the longitudinal (x direction) length scale, L, is much larger than the transverse (y direction) length scale, H, such that $\epsilon = \frac{H}{L} << 1$. For reference, see Figure (2.2). The thinness assumption also leads to the simplifying assumption of rapid dilution of the gel by vaginal fluid exuded from the wall in the y direction such that the gel fraction, Φ, is a function of x only. Gel fraction is defined as the volume fraction of gel as prepared in the mixture of applied gel and diluting fluid. We also argue that the curvature of the wall is negligible, again due to the separation of length scales, and therefore phenomena such as traction forces occurring at the vaginal wall act purely in the y direction.

The pressure field in the fluid caused by the force from the vaginal wall is developed using a one dimensional constrained continuum model. Therefore, local pressure (p) of the fluid is approximated as proportional to local deformation of the compliant wall (h) with a compliance parameter (M) such that $p = Mh$ [13]. The mass conservations stated in Eq (2.1) and (2.2) are derived from these assumptions. Their full derivation can be found in [76].

$$\frac{\partial h}{\partial t} + \frac{1}{2}\frac{\partial}{\partial x}\left[(M\frac{\partial h}{\partial x})m_2\right] = -q \tag{2.1}$$

$$\frac{\partial(\phi h)}{\partial t} + \frac{1}{2}\frac{\partial}{\partial x}\left[\phi(M\frac{\partial h}{\partial x})m_2\right] = \frac{\partial}{\partial x}(hD_{gw}\frac{\partial \phi}{\partial x}) \tag{2.2}$$

In these equations, the diluting boundary fluid flux, q, is included as a source term; $D_{gw} = 10^{-5}\frac{cm^2}{s}$ is the mutual diffusion coefficient of the water and the gel [77], ρ is equivalently the density of the water or gel, and $h(x,t)$ is the distension of the vaginal wall relative to the plane of symmetry. The compliance parameter is calculated as elasticity divided by tissue thickness ($0.5cm$ for the vaginal wall), $M = \frac{E}{T} = 20\frac{kPa}{cm}$ [75]. Shear rate ($\dot{\gamma}$) and stress (τ) are related to one another through the variable m_2 which is analogous to viscosity.

$$m_2 = \int_{-h}^{h} \left[\int_{-h}^{y} F(\tau_{xy}) y dy \right] dy \tag{2.3}$$

$$\dot{\gamma} = \tau_{xy} F(\tau_{xy}) \tag{2.4}$$

The shear stress (τ_{xy}) is calculated as in Szeri et al. (2008)[75].

$$\tau_{xy} = y(M\frac{\partial h}{\partial x} - \rho g) \tag{2.5}$$

The x balance of linear momentum yields an equation for the velocity in the x direction, u_1, as done previously [75, 77]

$$u_1 = \int_{-h}^{y} F(\tau_{xy}) \left[M\frac{\partial h}{\partial x} \right] y dy. \tag{2.6}$$

From the incompressiblity condition, a differential equation for the velocity in the y direction, u_2, is

$$\frac{\partial u_2}{\partial y} = -\frac{\partial u_1}{\partial x}. \tag{2.7}$$

Three separate compartments are defined in the drug transport model. The first is the gel located within the lumen of the vaginal canal. The second is the epithelium which is about 20μm thick containing cells that are uninfectable by HIV and no vasculature. Finally, the stroma is a layer composed of primarily connective tissue containing infectable cells and approximately 10% vasculature by volume; it is about 2500-3000 μm thick. Each compartment has its own mass conservation/ transport equation connected by continuous mass flux and concentrations boundary conditions with partition coefficients. In addition, the model includes a dilution term in the gel and a deformation term in the stroma (the last terms in equations (2.8) and (2.10)). Driving the convection of the drug in the lumen are the gel spreading velocity components (u_1 and u_2) which also couple the drug transport model to the gel motion model. Therefore, the drug transport equations for each compartment are as follows.

In the lumen ($y = 0$ to $y = h$):

$$\frac{\partial c}{\partial t} = D_L \left(\frac{\partial^2 c}{\partial x^2} + \frac{\partial^2 c}{\partial y^2} \right) - \left(u_1 \frac{\partial c}{\partial x} + u_2 \frac{\partial c}{\partial y} \right) - c \left(\frac{|q|}{h} \right). \tag{2.8}$$

In the epithelium ($y = h$ to $y = h + h_E$):

$$\frac{\partial c}{\partial t} = D_E \left(\frac{\partial^2 c}{\partial x^2} + \frac{\partial^2 c}{\partial y^2} \right). \tag{2.9}$$

And in the stroma ($y = h + h_E$ to $y = h_{total}$):

$$\frac{\partial c}{\partial t} = D_S \left(\frac{\partial^2 c}{\partial x^2} + \frac{\partial^2 c}{\partial y^2} \right) - K_B c + \frac{1}{(h_{total} - (h + h_E))} \frac{\partial h}{\partial t} c. \tag{2.10}$$

In Equations (2.8 - 2.10), $c(x, y, t)$ represents the local drug concentration. All drug transport parameters in these equations (See Table (2.1)) were taken directly from the model by Gao et al. (2015) [30]. The last terms in Equations (2.8) and (2.10) are corrections to account for mass conservation. In the gel, we assume that fluid flux from the wall changes the local concentration uniformly in the y-direction due to the thinness of the layer and slowness of the flow. The drug transport equation is then corrected by adding in a term based on the time rate of change of concentration in the absence of convection or diffusion.

In the stroma, we assume that the tissue has elastic properties due to its structure and thickness, which is roughly one hundred times that of the epithelium. Stromal tissue thereby compresses in response to surface forces from the compliant vaginal wall. Again due to the small wall curvature, we assume that stress in the solid acts in the y-direction only. This allows us to write the one dimensional mass conservation correction (i.e. the last term) seen in Equation (2.10).

The model has been simplified to a greater degree in a few more ways. The length of the canal is taken to be 40 cm which is greater than the anatomical length of the vagina [5]. This allows us to neglect the effects on flow from the introitus (vaginal opening) and fornix (where the vaginal canal terminates) of the canal. Pressure can be taken as atmospheric at both ends as it is at the outer boundaries of the gel in the model. Depending upon the elapsed time and the site of initial gel placement, for larger times the net extent of bilateral gel spreading here could exceed that of the canal. However, the goal of this model is to make quantitative comparisons - for varying values of gel rheology, inserted volume, loaded drug concentration, and vaginal fluid production. These comparisons should not be significantly altered versus those for flows constrained at either end. The effects of gravity have been neglected for two main reasons: (1) the orientation of the vaginal canal will vary as a woman changes position, walks, etc.; and (2) the quantitative effets of gravity on flow are small when compared with those of vaginal squeezing forces, and have been analyzed previously [75, 2]

Parameter	Description	Value
D_E	Diffusion coefficient of tenofovir in epithelium	$7 \times 10^{-8} \frac{cm^2}{s}$
D_S	Diffusion coefficient of tenofovir in stroma	$4 \times 10^{-7} \frac{cm^2}{s}$
D_L	Diffusion coefficient of tenofovir in lumen gel	$6 \times 10^{-6} \frac{cm^2}{s}$
K_B	Blood loss rate constant	$3.39 \times 10^{-5} s^{-1}$
h_E	Epithelium thickness	$0.02cm$
h_S	Stroma thickness above max height of the gel	$0.28cm$

Table 2.1: Values of thicknesses of mucosal layers and mass transport transport parameters for tenofovir are given here as experimentally determined by Chuchuen. Note that the drug has different diffusion coefficients in the epithelial and stromal layers, which is due to their different structures [16].

Initial Conditions

The velocity of the gel in the bolus is initially set to zero when it is placed at the center of the lumen. Initial gel dilution is taken as uniform and is expressed as the initial gel fraction, ϕ_i. The drug concentration is also taken to be uniform initially and is taken to be either $2 \times 10^7 \frac{ng}{mL}$ or $1 \times 10^7 \frac{ng}{mL}$. The smaller concentration corresponds to that of the CAPRISA 004, VOICE, and FACTS clinical trials [41, 53, 24]. The higher concentration would maintain the same mass of drug as in the trials when applied in a $2mL$ bolus.

The initial shape of the bolus depends on the given initial volume according to Szeri et al. (2008) [75]:

$$V_b = 2ABC\sqrt{\pi} \tag{2.11}$$

$$h(x, t = 0) = h_\infty + B \exp\left[-\left(\frac{x}{A}\right)^2\right]. \tag{2.12}$$

Here, V_b is the total initial bolus volume, $C = 3cm$ is the width of the vagina (in the z direction) [5], $B = 0.25cm$ is the initial maximum height of the bolus measured from the centerline [76], and A is the bolus half-width value. The source of the $h_\infty = 0.1b$ term is the assumption of a flooded boundary condition in the lumen. The details of the initial bolus shape are quickly forgotten by the gel as it flows [75]. Though the fluid outside of the central bolus would be water only, it is mathematically convenient to take the fluid as having a uniform gel fraction throughout the domain. At the far ends of the domain, the fluid is not

Ingredient concentrations (% by weight)	Universal Placebo Gel	IQB 3002	IQB 4012
Hydroxyethelcellulose	2.70	2.10	1.00
Glycerol	-	2.50	2.50
Carbopol	-	0.25	1.00
Tenofovir	-	-	1.00
IQP - 0528	-	1.00	1.00
Osmolality (mmol/kg)	298	380	360
pH	4.5	6	6

Table 2.2: Gel compositions as well as each gel's osmolality and pH [49, 35].

subject to pressure or wall shearing and is therefore insensitive to viscosity differences. In contrast, the drug concentration is set to zero outside of $|x| > A$ so that all of the drug is contained within the main volume of the bolus.

The gels used in this kind of application are commonly shear thinning and can be modeled by a Carreau-like constitutive equation fitted to experimental data [75, 77]. Three candidate gels are examined in this work. Two were prototype microbicide gels (IQB-3002 and IQB-4012) and one was the hydroxyethylcellulose gel used in virtually all vaginal microbicide trials to data (Universal Placebo Gel). Table 2 gives gel compositions, osmolalities, and pH values. The rheological characterizations were performed by our research collaborators [29] at body temperature (37°C) using a constant stress protocol on a TA Instruments (Newcastle, DE) model AR 1500ex rheometer, with a 4° cone and 20 cm plate configuration. Shear rates ranged from 10^4 to 250s^{-1}. Although these shear strain rates had a peak value of 250s^{-1}, the shear strain rate distribution during gel spreading has an order of magnitude smaller peak value than this [46]. Data were fit with this lower, biophysically relevant upper bound, to avoid any effects of gel slippage at the cone and plate surfaces at higher shear rates. Residual stresses of the gels were measured, as surrogates for yield stress, by stress relaxation experiments in a Brookfield 5HB DV-III Ultra rheometer with a CPE-40 cone [56]. This enabled determination of the values of m, m_0 and n in the Carreau-like constitutive model as functions of serial dilutions of the original gel.

From Eq (2.4), shear rate of the gel ($\dot{\gamma}$) is related to the shear stress (τ_{xy}) through a function F:

$$F(\tau_{xy}) = \frac{1}{m_0} + \frac{1}{m}\left(\frac{|\tau_{xy}|}{m}\right)^{\frac{1-n}{n}}. \tag{2.13}$$

The fitted viscosity parameters n, m, and m_0 for each gel depend on the dilution of the gel (ϕ) as shown in Table (2.3).

	Universal Placebo Gel	IQB 3002	IQB 4012
m_0	$916.8\exp(-\left[\frac{1.123-\phi}{0.2915}\right]^2)$	$0.08735\exp(9.079\phi)$	$3.111\exp(7.086\phi)$
n	$0.6905(1-\phi)^3 + 1.9704(1-\phi)^2 - 0.9217(1-\phi)+0.6601$	$-0.1282\phi + 0.4287$	$-0.3009\phi + 0.5603$
g	$27936.6(1-\phi)^3 - 18848.0(1-\phi)^2 + 1847.4(1-\phi) + 382.1$	NA	NA
m	$\frac{m_0}{g^{1-n}}$	$179.3\phi - 103.5$	$286.6\phi - 190$
Range of gel fraction tested	0.75 - 1.00	0.70 - 1.00	0.70 - 1.00

Table 2.3: Experimentally determined Carreau-like fluid rheological parameters. Expressions were obtained using polynomial curve fitting.

In addition to relating the shear rate to shear stress, $F(\tau_{xy})$ is a useful relation because $\frac{1}{F(\tau_{xy})}$ represents what we call the effective viscosity of the gel. This means that in order for a Newtonian fluid to behave similarly under the same conditions, its viscosity would have to match the effective viscosity of the Carreau-like fluid. This allows us to compare the behavior of the Carreau-like fluids within the context of more familiar Newtonian fluids [75].

2.2 Simulation Construction

We have divided the process of tenofovir delivery into two distinct models (gel transport and drug transport) and accordingly implement two mostly separate numerical solvers that are connected by nodal velocity field values in the vaginal canal. Gel spreading is solved using a finite difference method, while drug transport is solved using finite elements with a Forward Euler correction step.

Gel Spreading Finite Difference Solver

As the gel spreading equations have been reduced to a one dimensional form, they can be easily expressed on a simple linear domain of constant grid spacing. Spatial derivatives are approximated by centered differences. The time component of the partial differential equations is solved using Backward Euler. An adaptive time step addresses stiffness at early times and maintains convergence. Time step size is controlled by the requirement that total

gel volume be conserved within a given tolerance. Specifically, we require that between two sequential time steps,

$$\Delta\{\frac{1}{c}\int_{-x_\infty}^{x_\infty} h\phi dx\} \leq (threshold). \tag{2.14}$$

In the hyperbolic term of equations (2.1) and (2.2), the m_2 parameter changes rapidly from a shear thinning fluid to a Newtonian fluid based on the gel fraction and therefore has shock-like properties. To address spurious oscillations caused by this issue, we use an upwinding method that takes spatial derivatives only on upstream nodes of a three node stencil, where the upstream direction is based on the sign of the gradient, $\frac{\partial m_2}{\partial x}$.

A conservation check routine in the solver determines that over 8 hours of simulated time total gel volume and total fluid volume are conserved within 0.1% of their respective initial values.

Drug Transport Finite Element Solver

Relative transport timescales determine roughly how often the drug transport solver should iterate within the encompassing gel spreading solver time loop. A time scale for gel spreading is $t_s = \frac{L}{U} = \frac{10^{-1}}{10^{-5}} = 10^4$ seconds, where U is an approximate flow velocity. For drug transport we use the time scale of the diffusion length, $t_d = \frac{T^2}{D} = \frac{(10^1)^2}{10^{-8}} = 10^6$ seconds, where T is the vaginal tissue thickness scale and D is the tissue diffusion coefficient. Comparing these time scales, we conclude that the drug transport problem unfolds at a considerably slower rate which allows for a different pace of time-stepping. In our simulations, it occurred approximately every 10^2 iterations of the gel spreading solver.

The convection-diffusion equations (2.8,2.9,2.10), are solved using 4-node, linear isoparametric quadrilateral finite elements in space and Backward Euler in time. After each iteration of this step, the dilution and deformation correction equations included in Equations (2.8) and (2.10), are solved using a simple Forward Euler scheme on each node.

As time progresses, the vaginal wall moves and the compartment domains change shape. Nodes are placed at constant, regularly spaced intervals in the x-direction. In the y-direction, the number of nodes per compartment remains constant and their spacing scales with the height of each compartment at each time step. At any given x-position, the y-spacing of nodes is uniform within each compartment, though different between compartments, such that a given node always remains within the same compartment. This node placement approach allows that the velocity field calculated on the finite difference mesh from equations (2.6) and (2.8) does not require any interpolation for use in the finite element method.

Mesh deformation is not accounted for as additional degrees of freedom on the mesh. Instead, the drug concentration field is interpolated onto the new mesh before each iteration. The error introduced by the interpolation step is acceptable so long as the mesh deformation is small between iterations. We ensure a controlled magnitude of deformation by adapting the drug transport time step according to the translation speed of the vaginal wall interface, calculated as $\frac{\partial h}{\partial t}$.

Before the transient gel spreading approaches equilibrium, the transport of drug in the lumen is convection driven and the x-direction Péclet number for drug transport in the lumen, $Pe_x = \frac{u_1 L}{D_L}$, is large. To damp potential numerical oscillations, a streamwise upwind Petrov-Galerkin method is applied in the lumen. We choose to adopt in our implementation the added-diffusion interpretation of upwinding on finite elements. As such, diffusion is added to the x-direction values of the stiffness matrix in the lumen compartment according to the grid Péclet number $Pe_{\Delta x} = \frac{u_1 \Delta x}{D_L}$ and the optimal grid diffusion equation for a grid of uniform spacing [10] ,

$$D_{Grid} = \frac{\Delta x}{2}\{\coth(Pe_{\Delta x}) - \frac{1}{Pe_{\Delta x}}\}. \tag{2.15}$$

A drug conservation check is implemented on the FEM mesh at each time step. Over 8 hours of simulation time, total drug quantity change is less than 2% for all experimental runs. Moreover, conservation improves at later times when concentration gradients are relaxed.

2.3 Comparison of gels

Simulations were performed for the three gel with varying levels of initial dilution by ambient vaginal fluid, diluting fluid flux from the walls, gel bolus volume, and initial loaded drug concentration. A total of 36 cases were considered.

Effective viscosity as a function of applied shear rate and dilution is shown in Figure (2.3). There are clear contrasts between the gels. Dilution by 25% causes about a 1 log decrease in effective viscosity per gel at low shear rates. As shear rate increases, the relative decrease in effective viscosity diminishes for gels IQB-3002 and IQB-4012 but diminishes less for the Universal Placebo gel. At low shear rates, flow behavior approaches that of a Newtonian fluid where the (relatively high) viscosity is determined by the plateau or zero shear limit viscosity m_0. At shear rates higher than those of the plateau region, effective viscosity decreases with increasing shear rate, i.e. the behavior is shear thinning; this is consistent with the Carreau-like fluid model in which the extent of shear thinning is exponential (as in the Power Law model).

As discussed in previous work [75, 76, 30], the spreading behavior of the gel directly affects the delivery of drug into tissue, because it governs the contact area of the gel with the tissue surface. Thus, increased spreading leads to increased drug mass delivered, as seen in Figure (2.4). Here, 2 mL boluses of all three gels, with 1% initial drug concentrations, undergo maximum net dilution (initial dilution and subsequent dilution from the wall flux). Gel spreading is defined via the spread length (defined as four standard deviations of the bolus height profile which is interpreted as a probability density function [75]). All three gels (holding other conditions constant) spread at different rates at small times, but over time approach the same steady state. This difference in early spreading behavior has a noticeable effect on the amount of drug that is ultimately delivered. Drug concentration gradients are highest at early times with relatively rapid drug diffusion into tissue. As the diffusion

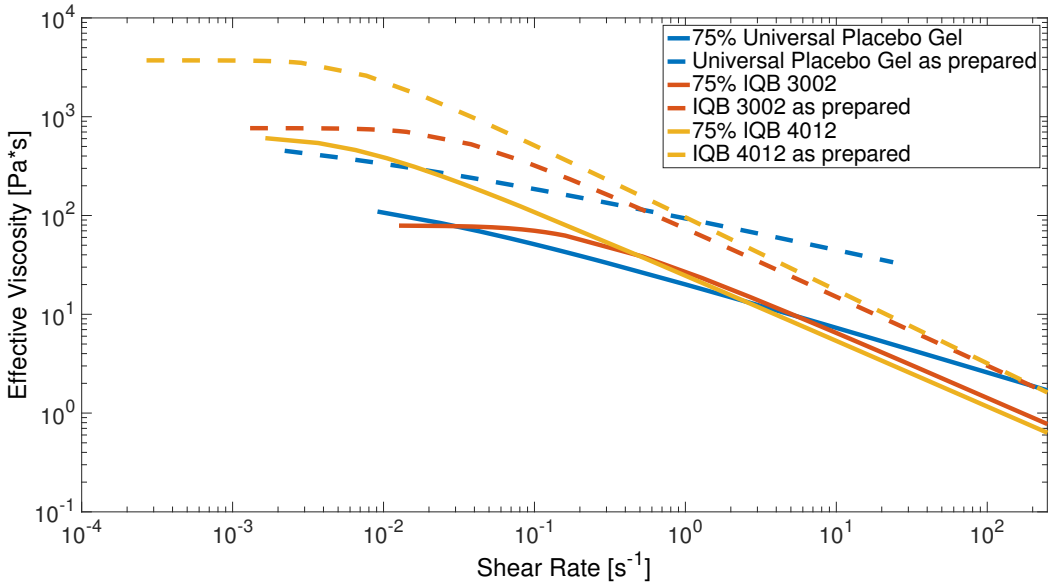

Figure 2.3: Apparent viscosity of a Carreau-like fluid depends on the applied shear rate as well as the dilution of the gel.

gradients lessen, increases in spread length have a diminished effect on drug transport. Thus, controlling the spreading behavior at early times has a significant effect on net drug delivery.

2.4 Relative importance of shear thinning and gel dilution

Shear thinning and dilution have significant effects on the mechanics of gel spreading. The characteristic curves, which show the effective viscosity of the gel for all x-locations in the gel at a certain time, describe this interesting narrative. Because each curve is sensitive to gel volume fraction and because that fraction is a function of position, we must choose a reference location for analysis here. The point at which shear rate is maximized closely follows the leading edge of the spreading front and is therefore a natural choice.

At early times when the gel has not yet spread appreciably, the shear rates at the edges of the bolus are quite high, causing the gel to exhibit strong shear thinning behavior as seen in Figure (2.5). As the bolus begins to spread out, the shear rates decrease relatively quickly. Fifteen minutes into the simulation, the gel is exhibiting primarily Newtonian behavior (associated with the low shear-rate plateau in Fig (2.3)) at a relatively high viscosity. At later times, boundary dilution decreases the zero shear rate viscosity such that the flow is still Newtonian but with a lower effective viscosity. From this, we understand that early spreading behavior, which is strongly tied to the ultimate amount of drug delivered into

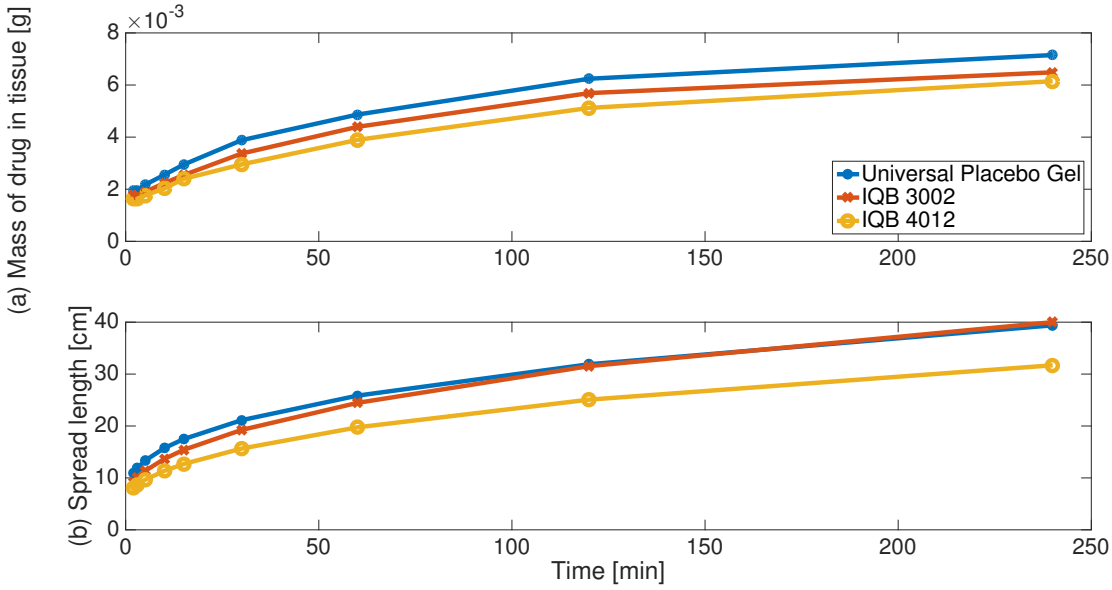

Figure 2.4: Mass of drug delivered (a) and spread length (b) as functions of time. All simulations are for $2mL$ boluses with an initial drug concentration of 1%. The gels have an initial gel volume fraction of 85%, and fluid flux from the walls is included at a rate of -3.5e-9$\frac{m}{s}$.

tissue, is influenced by the gel's shear thinning characteristics while later spreading behavior is dominated by dilution.

2.5 Varying simulation factors

The three clinical microbicide efficacy trials (Phases IIb, III) of tenofovir gel all used used the same 1% tenofovir gel applied at 4 mL. It is therefore instructive to consider the situation in which the volume is varied for this gel, but loaded drug concentration is conserved, not total drug mass, as above. Results are illustrated in Figure (2.6). Here, the 4 mL bolus contains twice the initial mass of drug as compared to the 2 mL bolus. Unsurprisingly, the mass of drug delivered into tissue is higher (about 20%) at one hour for the 4 mL bolus, due in large part to the increased spreading at early times. At later times, this relative difference diminishes, e.g. reaching about 9% at three hours. However, doubling the size of the bolus (and the initial dose of drug) does not double the mass of drug that is ultimately delivered into the tissue. This suggests a tradeoff between the size of the bolus and the proportion of the initial loaded drug mass in the gel that enters tissue. The smaller bolus benefits from having a thinner layer of gel, with steeper concentration gradients and reduced diffusion distance for drug migrating to the tissue.

Further interesting results are associated with fluid that is naturally present in the lumen.

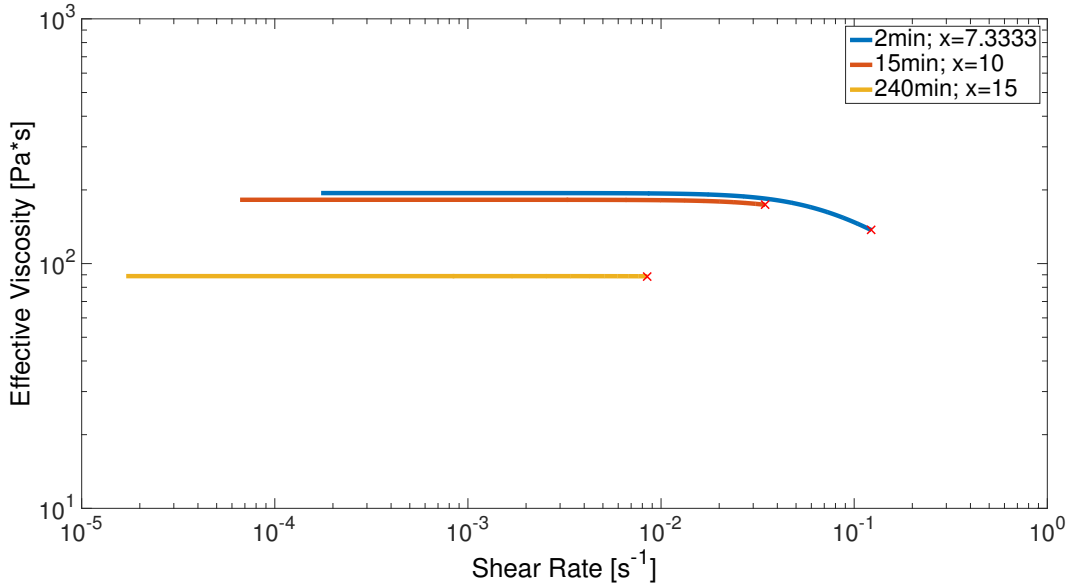

Figure 2.5: Curves of effective viscosity as a function of shear rate at the location of maximum shear rate for a simulation of a 2 mL bolus of IQB 3002 with no initial dilution and including a fluid flux from the wall of -3.5e-9$\frac{m}{s}$. See Figure 2.3.

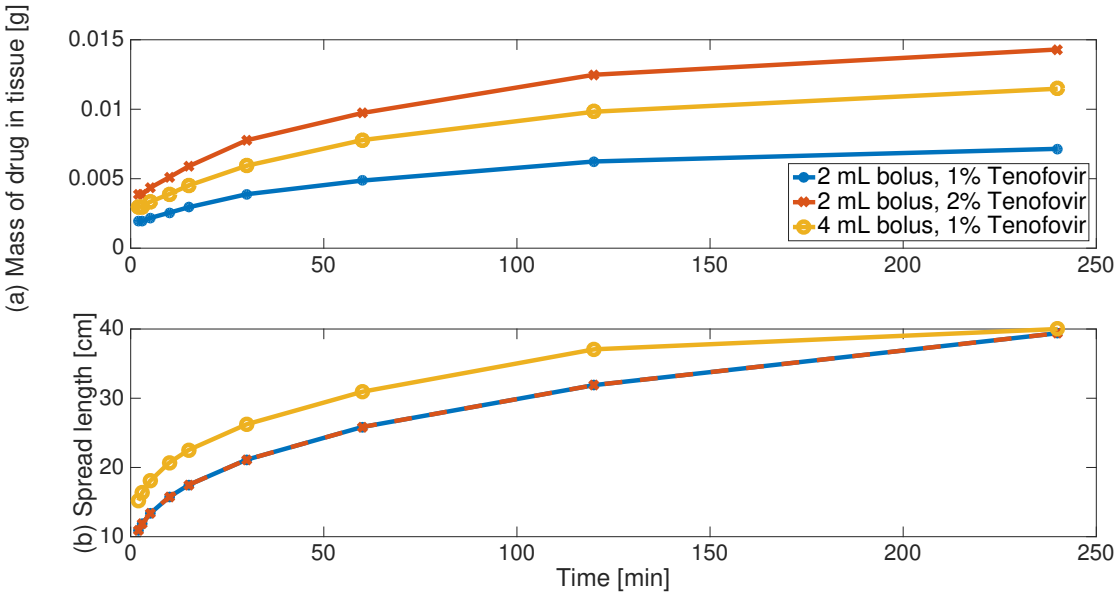

Figure 2.6: Mass of drug delivered (a) and spread length (b) as functions of time. The results are shown for the international placebo gel with an initial gel volume fraction of 85% and including fluid flux from the walls at a rate of -3.5e-9 $\frac{m}{s}$.

There is likely some ambient fluid distributed along the vaginal canal prior to application of the gel. Measurements of such fluid have found 0.5 - 0.75mL at any given time of the day with an average production rate of approximately 6 mL/day [57]. An initial gel fraction (defined as the percent of fluid by volume which is comprised of the original gel as prepared) of 85% means about 0.35mL or 0.7mL of ambient fluid for the 2mL and 4mL bolus simulations respectively. We used a maximum vaginal fluid production rate of 3.5×10^{-9}m/s, which produces a little over 7mL of fluid per day. Serial gel dilutions with vaginal fluid simulant in the rheological evaluations of the gels included this upper bound on initial dilution. Intuitively, initial dilution per se (all other factors being equal) will increase the spread length because initial viscosity will diminish. This increased spreading is promising for increasing drug delivery; however, dilution also decreases the concentration gradient which is a driving force in the drug delivery. Consequently, we see in Figure (2.7) that including initial dilution decreases the total amount of drug delivered to tissue in four hours by a significant amount. Also of interest is how continuous production of fluid impacts the spreading behavior and drug delivery. Again due to the rheological nature of the Carreau-like fluids, increasing fluid flux increases spreading. However, the effect here on drug delivery is more complex. In Figure (2.8), we see for gel IQB-3002 that although fluid flux decreases the concentration gradient, it actually increases the amount of drug which is delivered into the tissue over a four hour simulation if initial dilution is not included. This is in direct contrast to what is seen in Figure (2.7) for the Universal Placebo Gel, for which including fluid flux decreases the amount of drug delivered into tissue for the international placebo gel. Clearly, the effects of fluid flux are dependent on the specific gel being studied.

2.6 Conclusions

In this chapter, we developed important techniques and learned of several factors affecting the drug delivery problem. Among these is how to incorporate two distinct phenomena (gel spreading and diffusive drug transport) into a single numerical model. In order to do this, we paid careful attention to length scales and time scales which allows us to create an efficient multi-step, multi-domain solver. In particular, the long and thin geometry allows us to make the Reynolds lubrication approximation which greatly simplifies the equations used to solve for gel flow. This separation of length scales also allows us to simplify the movement of water through the lumen domain such that we only need to solve for its transport in the x-direction. With respect to time scales, the gel spreading occurs much faster than the drug diffusion, so we are therefore able to avoid solving for drug transport at every gel spreading step. Thus, the separation of time scales greatly saves on computation time.

With the model constructed, we were able to investigate how the rheological characteristics of the gel could influence the ultimate amount of drug which is delivered into tissue. Of particular interest were the shear-thinning behavior as well as the response of a gel to dilution. We learned that at early times when the shear forces on the gel are greatest, the rate of gel spreading is dominated by the shear-thinning of the gel which allows the bolus

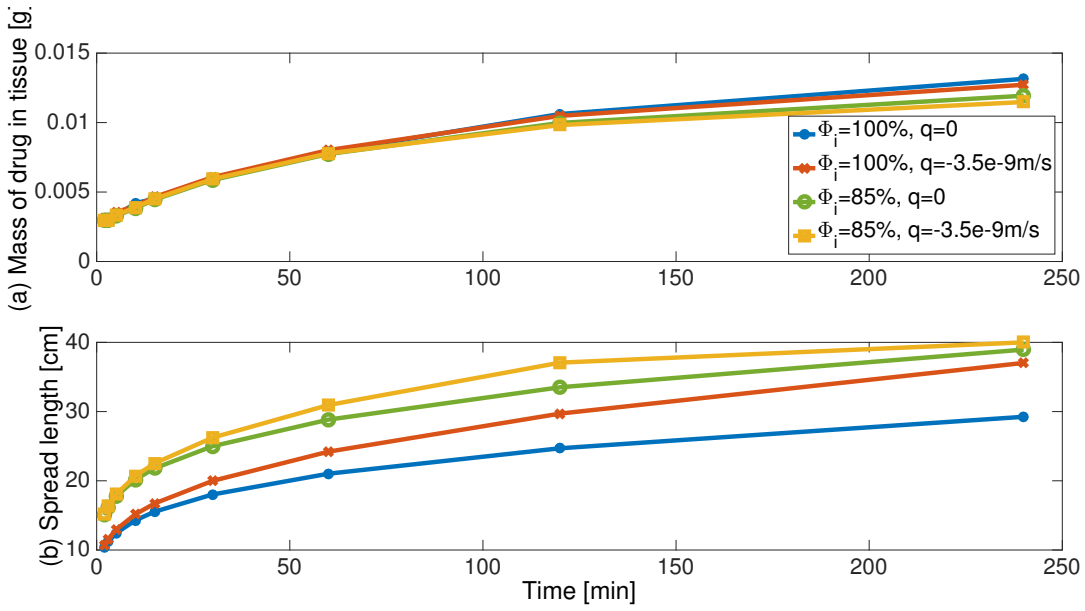

Figure 2.7: Mass of drug delivered (a) and spread length (b) as a function of time. The results are shown for $4mL$ boluses of the universal placebo gel with 1% tenofovir.

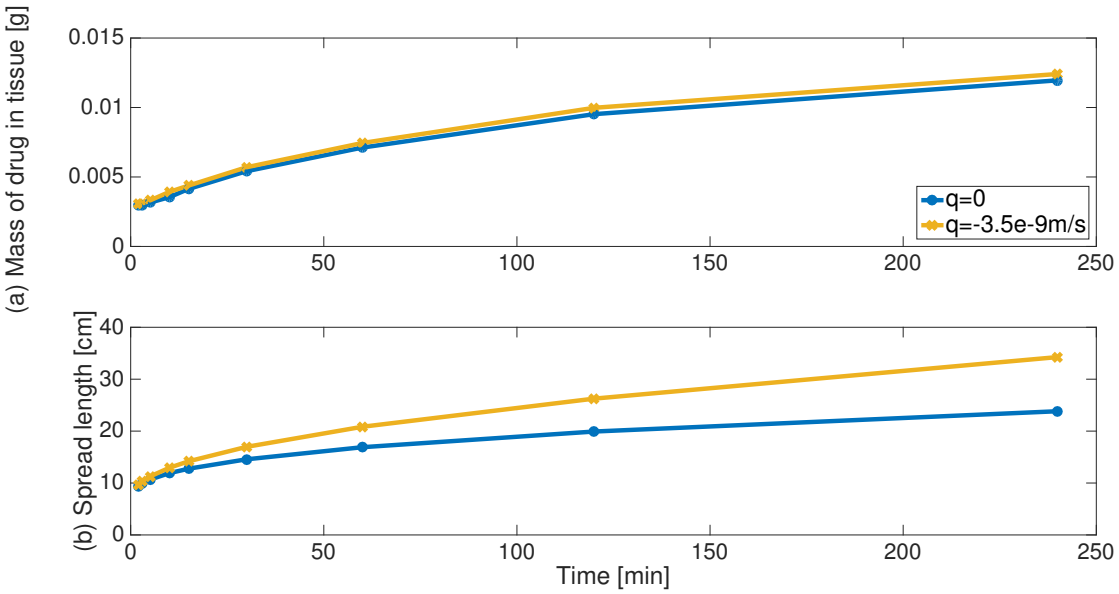

Figure 2.8: Mass of drug delivered (a) and spread length (b) as a function of time. The results are shown for $4mL$ boluses of IQB 3002 with no initial dilution.

to spread faster. This promotes greater amounts drug being delivered into tissue. Later spreading behavior is dominated by boundary dilution when the gel behaves primarily as a Newtonian fluid with progressively smaller viscosities. The progressive dilution of the gel reduces the concentration gradient of the drug between the lumen and the stroma; the reduced concentration gradient reduces the amount of drug that arrives into tissue.

It is interesting to note that the effects of boundary dilution on drug delivery are specific to the gel being studied. At early times, the boundary dilution aids the spreading process which we know is tied to the amount of drug delivered into tissue. If the effects of boundary dilution on early spreading are stronger than its effects on diluting the concentration of the drug in the lumen, then boundary dilution can improve drug delivery behavior as is seen for IQB 3002. However, the effects are reversed for the universal placebo gel indicating that a thorough understanding of the rheological characteristics of the specific gel to be used are significant.

In this study, we assumed uniform initial dilution and a constant value of fluid flux into the lumen. Although this is sufficient for an initial look into how dilution can affect the drug delivery problem, it is unlikely that natural fluid production would actually follow this pattern. Moving forward, we develop a more nuanced model of fluid flux including interactions between the gel and tissue based on osmolarity. A deeper understanding of boundary flux then suggests a sophisticated way to engineer a gel that would capitalize on the understanding of how to maximize drug delivery to tissue that was developed here.

Chapter 3

Osmolarity and its Effect on Drug Transport

In the previous chapter, we focused exclusively on gels as a drug delivery vehicle for a vaginally applied anti-HIV microbicide. One of our primary avenues of inquiry was into how biologically produced fluid will dilute the gel affecting both the concentration difference of the drug on its way into the body and the rheological properties of the gel as it spreads along the lumen wall. For lack of a better model, we assumed in Chapter 2 a constant rate of fluid dilution based on the average woman's daily production rate.

Though sufficient for a first look in Chapter 2 to illustrate factors influencing drug delivery, we are eager to explore how factors affecting biological fluid production would play into the drug delivery problem. Osmolarity of the drug solution was an obvious choice to investigate first as it is one of the most well known drivers of solvent transport across a permeable membrane. To begin to study this phenomenon as it applies to the drug delivery problem, we reduce it into its simplest form to create a workable model.

3.1 Coupled Solute and Solvent Transport

We begin by defining a system composed of two compartments (the body and the lumen) separated by a permeable membrane (e.g. the cell membranes of cells lining the canal wall). The contents of the two compartments are well mixed and are composed of two different solutes with water as the solvent. The solutes and solvent are all free to cross the permeable membrane. We expect that, over time, the solvent and solutes will reposition across the membrane so as to achieve an equilibrium. See Figure (3.1) for reference.

Following the method outlined by Knocikova et al. (2014) [45], we define the volumetric flow of the solvent across the membrane from the lumen into the body as:

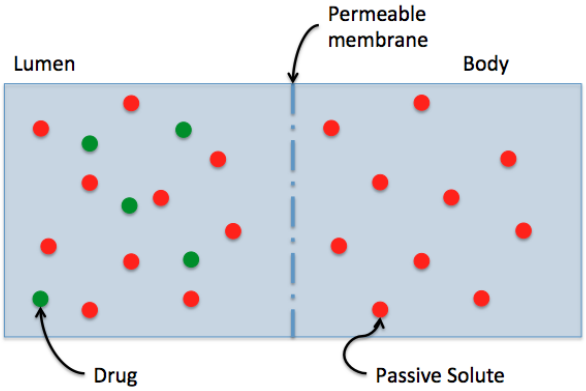

Figure 3.1: A schematic of the two-compartment, well-mixed problem setup.

$$Q = \frac{dV_l}{dt}, \tag{3.1}$$

where Q is a flow rate and V_l is the volume of fluid in the lumen compartment. Flow rate can also be defined using flux of water across the permeable membrane:

$$Q = \frac{j_w S_{mem}}{\rho_w}, \tag{3.2}$$

where j_w is the mass flux of water across the membrane, S_{mem} is the surface area of the membrane, and ρ_w is the density of water. The osmolarity of the solution inside the body is:

$$O_b = \sum n_i c_i, \tag{3.3}$$

where n_i is the number of species into which the i^{th} solute dissociates, and c_i refers to the concentration in moles liter of the i^{th} solute. As a simple example, if two moles of sodium chloride and one mole of glucose are dissolved into four liters of water, then the osmolarity of the solution will be calculated as follows:

$$O = 2(2)/4 + 1(1)/4 = 1.25. \tag{3.4}$$

Sodium chloride dissociates into two species when it dissolves, so two moles of NaCl dissolved into four liters of water results in an osmolarity of 1 Osm. Added to one liter of nondissociative glucose dissolved into the same four liters of water, the final solution has an osmolarity of 1.25 Osm.

The flux of solvent across the membrane can be written as:

$$j_w = \lambda(\Delta P - \Delta\Pi), \tag{3.5}$$

where λ is a coefficient of membrane permeability (defined in Eq (3.8)), ΔP is the difference in hydraulic pressure between the feed (lumen) and permeate (body) sides of the membrane, and $\Delta\Pi$ is the difference in osmotic pressures. Here, we assume that the difference in hydraulic pressures is negligible, and, according to van 't Hoff's law, osmotic pressure can be written as [47]:

$$\Pi = RTO, \tag{3.6}$$

where R is the universal gas constant, T is the temperature, and O is the osmolarity of the solution. Osmolarity can roughly be thought of as the inverse "concentration" of water. So if a solution on one side of a permeable membrane has a lower osmolarity than the other side, then it has a higher "concentration" of water which would lead to water flowing from the low osmolarity side to the high osmolarity side.

We can also define flux of solvent across the permeable membrane using Fick's first law as follows [26]:

$$j_w = \frac{D_w MW_w}{l}\Delta O, \tag{3.7}$$

where D_w is the diffusivity of water through the permeable membrane, MW_w is the molecular weight of water, and l is the thickness of the permeable membrane. Thus, combining Eqs (3.5) - (3.7), we define the coeffecient of membrane permeability to the solvent, λ as:

$$\lambda = \frac{D_w MW_w}{lRT} \tag{3.8}$$

If we combine these equations, we can now write volumetric changes as:

$$\frac{dV_b}{dt} = \frac{D_w MW_w((\sum n_i c_i)_b - (\sum n_i c_i)_l)S_{mem}}{l\rho_w}. \tag{3.9}$$

Due to mass conservation, the rate of change of the volume of fluid in the lumen is the opposite of that of the body:

$$\frac{dV_l}{dt} = -\frac{dV_b}{dt} \tag{3.10}$$

To track changes in concentrations over time, it is necessary to track solute particles in addition to the movement of solvent. If concentration is number of solute particles divided by volume, and both of those values are functions of time, then the following must be true:

$$\frac{dc}{dt} = \frac{1}{V}\frac{dn}{dt} - \frac{n}{V^2}\frac{dV}{dt}. \tag{3.11}$$

We know that the number of particles that move across the membrane will be:

$$(\frac{dn_x}{dt})_{dV=0} = -j_x S_{mem}, \tag{3.12}$$

where j_x represents the flux of solute x across the permeable membrane and according to Fick's law can be written as follows

$$j_x = -P(c_{x,l} - c_{x,b}) = \frac{D_x}{l}(c_{x,l} - c_{x,b}). \tag{3.13}$$

The permeability of the membrane with regards to the solute, P, is written as the diffusivity (D_x) divided by the thickness of the permeable membrane (l).

Thus, combining Eq (3.9,3.11,3.12) we completely describe the rate of change of concentration of an arbitrary, nonreactive solute in a volume of fluid subject to volumetric changes. The following is in the body:

$$\frac{dc_{x,b}}{dt} = \frac{1}{V_b}(-j_x S_{mem}) + \frac{n_x}{V_b^2}\frac{dV_b}{dt}. \tag{3.14}$$

Rewritten using Eq (3.13), Eq (3.14) becomes:

$$\frac{dc_{x,b}}{dt} = \frac{S_{mem}D_x}{l}\frac{c_{x,l} - c_{x,b}}{V_b} - \frac{c_{x,b}}{V_b}\frac{dV_b}{dt}. \tag{3.15}$$

3.2 Dimensional Analysis

If we assume two nondissociative solutes dissolved in the system (for example a drug and a passive solute representing naturally occuring biological compounds), then from the work done in Section (3.1), we have the following set of equations:

$$\frac{dV_l}{dt} = \frac{D_w MW_w S_{mem}}{l\rho_w}(O_l - O_b), \tag{3.16a}$$

$$\frac{dV_b}{dt} = -\frac{dV_l}{dt}, \tag{3.16b}$$

$$\frac{dc_{d,l}}{dt} = \frac{S_{mem}D_d}{l}\frac{c_{d,b} - c_{d,l}}{V_l} - \frac{c_{d,l}}{V_l}\frac{dV_l}{dt}, \tag{3.16c}$$

$$\frac{dc_{d,b}}{dt} = \frac{S_{mem}D_d}{l}\frac{c_{d,l} - c_{d,b}}{V_b} - \frac{c_{d,b}}{V_b}\frac{dV_b}{dt}, \tag{3.16d}$$

$$\frac{dc_{p,l}}{dt} = \frac{S_{mem}D_p}{l}\frac{c_{p,b} - c_{p,l}}{V_l} - \frac{c_{p,l}}{V_l}\frac{dV_l}{dt}, \tag{3.16e}$$

$$\frac{dc_{p,b}}{dt} = \frac{S_{mem}D_p}{l}\frac{c_{p,l} - c_{p,b}}{V_b} - \frac{c_{p,b}}{V_b}\frac{dV_b}{dt}, \tag{3.16f}$$

$$O_l = c_{d,l} + c_{p,l}, \tag{3.16g}$$

$$O_b = c_{d,b} + c_{p,b}. \tag{3.16h}$$

where the subscript b indicates the body compartment, l indicates the lumen compartment, d indicates the drug solute, and p indicates the passive solute.

We choose scaling values to create the following definitions to nondimensionalize the problem with stars denoting the corresponding dimensional value.

$$V_l^* = V_{l,0}^* V_l, \tag{3.17a}$$

$$V_b^* = V_{l,0}^* V_b, \tag{3.17b}$$

$$c_{d,l}^* = c_{d,l,0}^* c_{d,l}, \tag{3.17c}$$

$$c_{d,b}^* = c_{d,l,0}^* c_{d,b}, \tag{3.17d}$$

$$c_{p,l}^* = c_{d,l,0}^* c_{p,l}, \tag{3.17e}$$

$$c_{p,b}^* = c_{d,l,0}^* c_{p,l}, \tag{3.17f}$$

$$\Delta O^* = |\Delta O_0^*| \Delta O, \tag{3.17g}$$

$$t^* = \frac{l^* V_{l,0}^*}{S_{mem}^* D_d} t. \tag{3.17h}$$

We use the initial volume of the lumen compartment as a scale for volume and the initial concentration of the drug in the lumen to scale all concentrations. Note that the absolute value of ΔO_0^* is used to scale osmolarity in order to avoid inadvertently switching signs in equations if ΔO^* is negative.

The time scale is set by ensuring that the first term on the right hand side of Eq. (3.16c) is of the same order as the left hand side of the equation. Thus, we expect the rate of change of the concentration of the drug in the lumen to be of the same order as if the problem did not include any solvent transport. The effect of solvent transport is encapsulated in the second term on the right hand side.

Substituting in the dimensionless variables yields the following set of nondimensional equations equivalent to Eq. (3.16):

$$\frac{dV_l}{dt} = \frac{D_w MW_w |\Delta O^*|}{D_d \rho_w} \Delta O = F \Delta O, \tag{3.18a}$$

$$\frac{dV_b}{dt} = -F \Delta O, \tag{3.18b}$$

$$\frac{dc_{d,l}}{dt} = \frac{c_{d,b} - c_{d,l}}{V_l} - F \frac{c_{d,l}}{V_l} \Delta O, \tag{3.18c}$$

$$\frac{dc_{d,b}}{dt} = \frac{c_{d,l} - c_{d,b}}{V_b} + F \frac{c_{d,b}}{V_b} \Delta O, \tag{3.18d}$$

$$\frac{dc_{p,l}}{dt} = \frac{D_p}{D_d} \frac{c_{p,b} - c_{p,l}}{V_l} - F \frac{c_{p,l}}{V_l} \Delta O, \tag{3.18e}$$

$$\frac{dc_{p,b}}{dt} = \frac{D_p}{D_d} \frac{c_{p,l} - c_{p,b}}{V_b} + F \frac{c_{p,b}}{V_b} \Delta O. \tag{3.18f}$$

Here, we have two dimensionless groups: D_p/D_d, which is the ratio of diffusivities of the passive solute and the drug solute, and F, which is determined by the ratio of the time scale of diffusive drug transport to that of solvent transport across the permeable membrane at early times. F is defined in Eq (3.19). We expect the drug to move more slowly than the solvent, so in most cases, F is likely to be large.

$$F = \frac{D_w MW_w |\Delta O_0^*|}{D_d \rho_w} \tag{3.19}$$

Expanding on the ratio of time scales, we already determined a time scale for the set as Eq (3.17h). We made an assumption about the relation between the rate of change of the concentration of the drug in the lumen and the rate of diffusive drug transport across the permeable membrane. Another time scale naturally emerges from these equations from Eq (3.16a) which relates the rate of change of volume of the lumen to the initial difference in osmolarity across the permeable membrane. This timescale is:

$$t_2^* = \frac{l^* \rho_w V_{l,0}^*}{D_w MW_w S_{mem}^* |\Delta O_0^*|}. \tag{3.20}$$

If we used t_2^* to scale the set of equations, we would be assuming that all of the effects of interest in the problem occur on the same time scale as the volumetric flow of water across the membrane. However, we would like to examine problems that span the ranges of hypo- and hyperosmolar initial lumen conditions, so there will definitely be some situations in which this choice of time scale would be inappropriate. For example, in an iso-osmolar case, the time scale would be undefined.

Taking the ratio of Eq (3.17h) and Eq (3.20) evinces the dimensionless group, F. If this group is very small, then changes in drug concentration over time in the lumen or the body are driven almost exclusively by diffusion of the drug as $t^* << t_2^*$. In other words, diffusive transport of the drug is much faster than solvent flow across the membrane. However, if F is of order one or greater, then we expect drug concentration changes to be driven by volumetric changes of the compartments caused by motion of the solvent in addition to diffusion of the drug.

In Eq(3.18c-3.18f), the first terms on the right hand side represent the changes in concentration due to diffusive transport, and the second terms on the right hand side represent the changes in concentration due to volumetric changes from solvent transport.

Looking at this set, the first natural impulse is to look for a steady state solution dependent on the two dimensionless groups (F and D_p/D_d). However, these equations compose a nonlinear system. As such, finding a closed form solution is prohibitively difficult.

It is interesting to note, though, that they have the following natural properties stemming from mass conservation:

$$\frac{d}{dt}(c_{d,l} V_l + c_{d,b} V_b) = 0, \tag{3.21a}$$

$$\frac{d}{dt}(c_{p,l}V_l + c_{p,b}V_b) = 0, \tag{3.21b}$$

$$\frac{d}{dt}(V_l + V_b) = 0. \tag{3.21c}$$

Thus, if we assume that the system reaches an equilibrium state as time approaches infinity, then we have the following:

$$c_{d,l,0}V_{l,0} + c_{d,b,0}V_{b,0} = c_{d,l,\infty}V_{l,\infty} + c_{d,b,\infty}V_{b,\infty}, \tag{3.22a}$$

$$c_{p,l,0}V_{l,0} + c_{p,b,0}V_{b,0} = c_{p,l,\infty}V_{l,\infty} + c_{p,b,\infty}V_{b,\infty}, \tag{3.22b}$$

$$V_{l,0} + V_{b,0} = V_{l,\infty} + V_{b,\infty}, \tag{3.22c}$$

$$c_{p,b,\infty} = c_{p,l,\infty} = c_{p,\infty}, \tag{3.22d}$$

$$c_{d,b,\infty} = c_{d,l,\infty} = c_{d,\infty}, \tag{3.22e}$$

where the last two equations of the set represent the assumption of equilibrium as time approaches infinity. By substituting Eq (3.22c-3.22e) into Eq (3.22a) and (3.22b), we find the following conditions on final concentrations of the solutions:

$$c_{d,\infty} = \frac{c_{d,l,0}V_{l,0} + c_{d,b,0}V_{b,0}}{V_{l,0} + V_{b,0}}, \tag{3.23a}$$

$$c_{p,\infty} = \frac{c_{p,l,0}V_{l,0} + c_{p,b,0}V_{b,0}}{V_{l,0} + V_{b,0}}. \tag{3.23b}$$

In terms of osmolarity, the two equations above collapse into a single equation:

$$O_\infty = \frac{(c_{d,l,0} + c_{p,l,0})V_{l,0} + (c_{d,b,0} + c_{p,b,0})V_{b,0}}{V_{l,0} + V_{b,0}}. \tag{3.24}$$

Although concentrations at late times are certainly of interest, we are more interested in knowing the mass of drug which has made it to its target in the body compartment. For that, we need to know final volume ratios which we can only determine numerically.

3.3 Results

The following results were obtained by solving the system of Eq. (3.18) using an explicit fourth order Runge Kutta method. Overall mass conservation was satisfied to a high degree of precision. Body osmolarity is taken as 300 mOsm/kg [57].

Parameter	Description	Value
$\frac{D_w}{l}$	Permeability of water through the membrane	$0.028\frac{cm}{s}$
$\frac{D_s}{l}$	Permeability of solute through the membrane	$1 \times 10^{-6}\frac{cm}{s}$
$\frac{V_{bath}}{V_{cells}}$	Ratio of the volume of the fluid bath to the fluid volume of the cells	8
O_{cells}	Initial osmolarity of fluid in cells	$0.300\frac{mol}{L}$

Table 3.1: Values of various constants used to replicate the figure produced by Knocikova et al. [45]. Values were chosen based on experience and best fit.

Validation of Model

By setting the initial drug concentration in the lumen compartment equal to zero (thereby eliminating Eq (3.18c) and (3.18d)), we are able to replicate closely the numerical simulation by Knocikova et al. [45] as shown in the comparison of Figures (3.2) and (3.3). Values for the constants were chosen using experience based on the expected order of magnitude and are listed in Table (3.1). As the exact values of constants used were not given in their paper, the level of agreement is remarkable. In addition, they were able to replicate their own experimental results which indicates that our dimensionless model also dependably tracks volumetric changes as solvent crosses the permeable membrane. This is significant as solvent transport is dependent on solute transport which is the primary variable of interest. If solvent transport is reliably predicted, then we assume that solute transport must also be predicted with a similar degree of accuracy.

Varying Osmolarity

Our next step was to examine varying levels of hyper- and hypo-osmolarity of the solution in the lumen compartment. We expect that if a hypo-osmolar solution is placed into the lumen, then water will flow from the lumen into the body compartment. This would focus the concentration of the drug in the lumen which would steepen the concentration difference between the lumen and the body compartments. We would therefore expect that the drug moves more quickly into the body compartment. Alternatively, we expect that if a hyperosmolar solution is placed into the lumen, then water will be withdrawn of the body compartment into the lumen. This would dilute the concentration of drug in the lumen which would result in less drug moving into the body.

Xiao et al (2017) [86] showed experimentally that a hypo-osmolar enema formulation delivered a larger dose of the microbicide into rectal tissue than a hyperosmolar formulation, confirming our expectations. In Figure (3.4), we verify the sense of these results using our numerical simulation. The dimensionless group, F, as well as the ratio of diffusivities of the

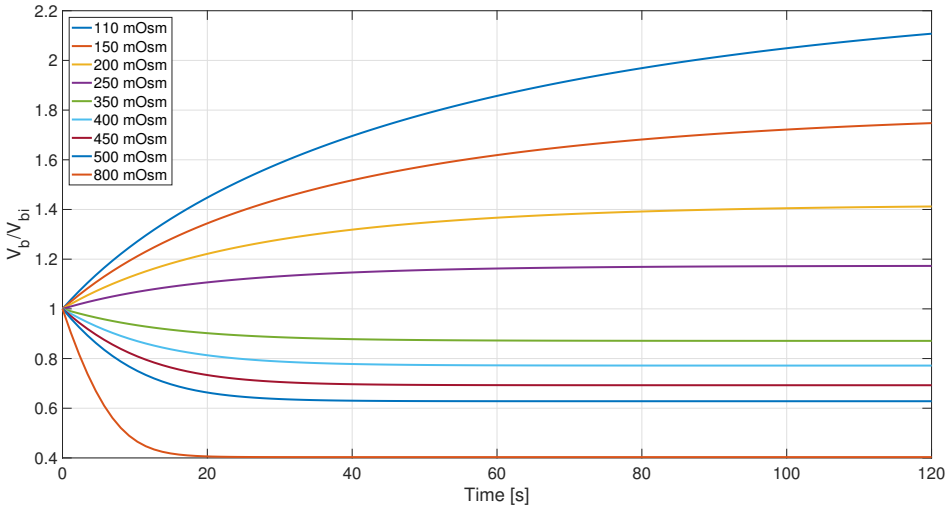

Figure 3.2: Normalized body compartment volume as a function of time. Labeled osmolarities are on the lumen side, and an osmolarity of 300 mOsm is iso-osmolar. Our dimensionless model dependably tracks volumetric changes as a function of osmolarity, despite the need to estimate unknown parameters in [45].

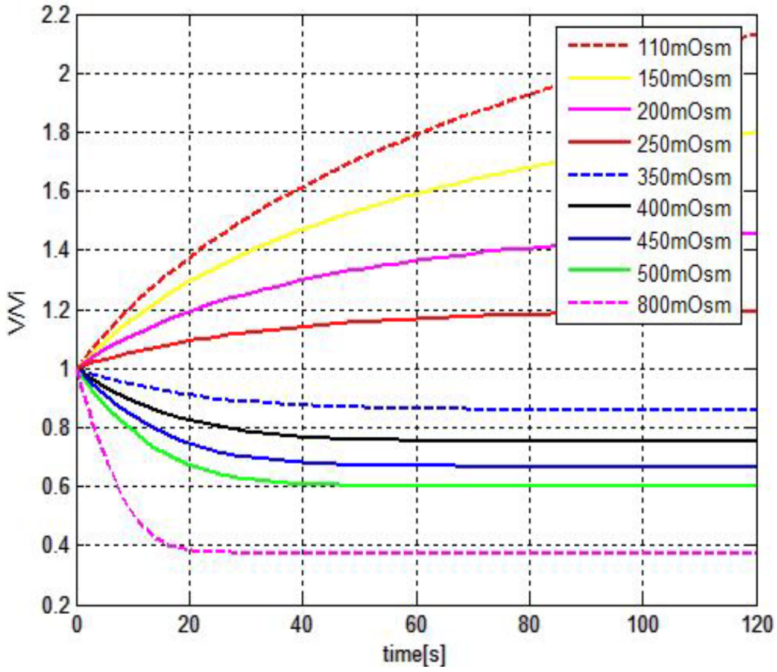

Figure 3.3: Original figure by Knocikova et al.[45]. A side by side comparison with the figure created by our simulations shows that our solution methods agree quite closely.

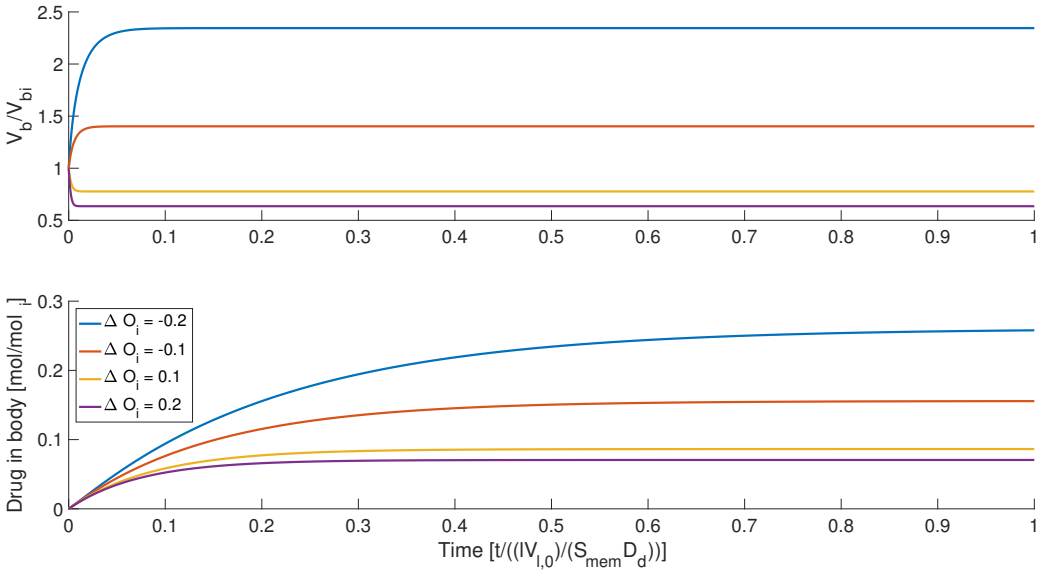

Figure 3.4: The top figure shows normalized body compartment volume due to solvent repartition as a function of time, and the bottom figure shows the normalized number of moles of drug that make it into the body compartment. The dimensionless group, F, as well as the ratio of diffusivities of the drug and the passive solute are both set equal to one. Positive ΔO indicates a hyperosmolar initial lumen condition.

drug and passive solute are set equal to one to ensure that the only effect being examined is changes in osmolarity. In other words, we assume that water transport across the permeable membrane initially occurs on the same time scale as diffusive transport, and the drug will move across the permeable membrane with the same ease as the passive solute.

Under the constraints of the assumptions made in the construction of this model, these results indicate that the improved delivery characteristics of the hypo-osmolar initial lumen condition are due to a steepened concentration difference across the permeable membrane as a result of the movement of solvent. The hypo-osmolar lumen condition drives water into the body compartment which simultaneously increases the concentration of the drug in the lumen and dilutes the concentration of the drug in the body compartment. Therefore, the more water that is driven into the tissue, the more drug will ultimately make it to its target. Of course, this statement comes with the caveat that the amount of water absorbed into the tissue would have to fall within safe ranges to prevent cells from bursting or experiencing other forms of tissue damage. We remind the reader that the compartments on either side of the membrane are regarded as well-mixed, at least on the time scale for crossing the membrane.

Varying F

The next effect that we looked at was how varying the dimensionless group, F, changes drug delivery. By examining Eq (3.18), we expect that varying F will influence how strongly the effects of solvent transport are felt on the rate of drug delivery into the body compartment. If F is very small, then we would expect that drug delivery would proceed as though solvent were unable to cross the permeable membrane, i.e. the drug concentration difference changes through diffusive transport only. On the other hand, if F is very large, then we expect that solvent transport across the permeable membrane has a strong effect on the drug concentration difference across the membrane. In the case of a hypo-osmolar lumen, water would flow into the body, steepening the concentration difference between the lumen and the body compartments. In the case of a hyperosmolar lumen, water would flow into the lumen, lessening the concentration difference. This hypothesis is confirmed in Figures (3.5) and (3.6).

We have already shown that a hypo-osmolar initial lumen condition increases the amount of drug delivered into the body compartment in Figure (3.4). When looking at a hypo-osmolar initial lumen condition in Figure (3.5), we see that values of F that are one or greater show large volumetric changes in the body compartment, i.e. a significant volume of water has moved from the lumen into the body. As a result, the amount of drug that arrives in the body compartment increases due to the steepened concentration difference. However, increasing F much beyond one comes with very little marginal benefit. Therefore, when formulating a drug delivery vehicle that can be made hypo-osmolar (e.g. enema or gel), the degree of hypo-osmolarity should be controlled such that F is at least equal to one (ideally greater than one) assuming that it falls within body safe limits.

On the other hand, looking at an initially hyperosmolar lumen condition in Figure (3.6), smaller values of F have increased amounts of drug delivered into the body compartment. Again, we emphasize that this is due to the directionality of the water transport. When water flows from the body into the lumen, as is the case here, the drug in the lumen is diluted which slows drug delivery. The marginal benefits of manipulating F for the hyperosmolar initial lumen condition are more significant than those of the hypo-osmolar case. Thus, when formulating a drug delivery vehicle that necessarily results in a hyperosmolar lumen (which is likely the case for a dissolving suppository or dissolving film), the value of F should be reduced to the greatest extent possible. There are two potential ways to do this. The first is to decrease the initial difference in osmolarity by reducing the amount of mass that is dissolved into the solution. The second (and not nearly as simple) method of reducing the value of F is to choose a drug with a large diffusion coefficient. However, this choice would also have the undesirable side effect of slowing down the transport of the drug into the body.

Varying D_p/D_d

Another interesting factor to manipulate is the ratio of diffusivities of the passive solute and the drug. The impact of this ratio is not immediately clear from a cursory inspection

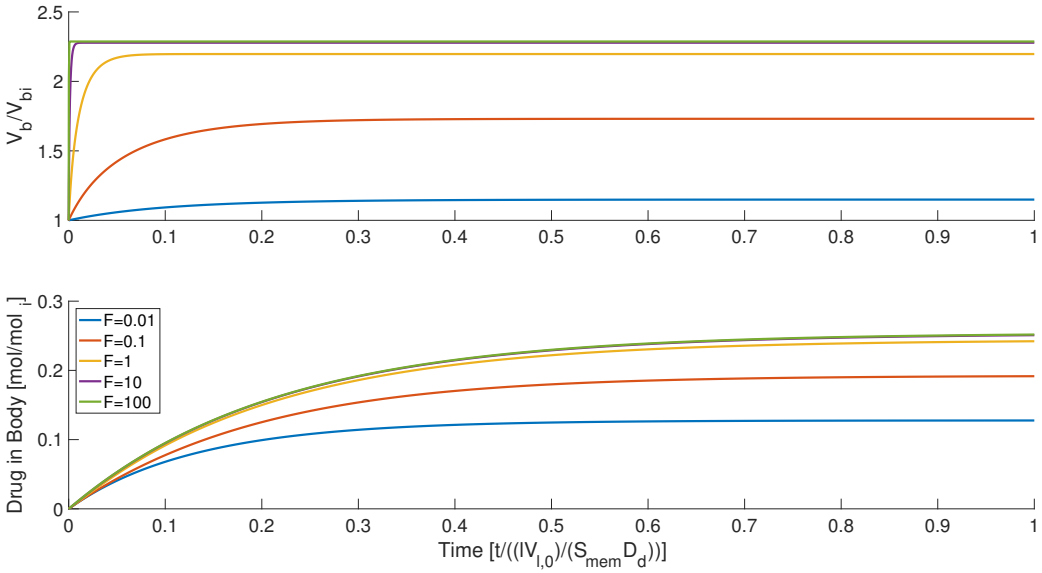

Figure 3.5: The top figure shows normalized body compartment volume as a function of time, and the bottom figure shows the normalized number of moles of drug that make it into the body compartment. The ratio of diffusivities of the drug and the passive solute is set equal to one, and ΔO is initially set to -0.2 (hypo-osmolar lumen). Increasing F beyond one results in little change.

of Eq (3.18f), but understanding it is critical as it is unlikely that the drug will have an identical diffusivity through a cell membrane to that of other solutes as we have thus far been assuming. Indeed, the compound most commonly used to manipulate the osmolarity of a gel or enema is common table salt which is much smaller and more easily transported through epithelium than bulky drug molecules.

In Figure (3.7), we see how manipulating the diffusivities with an initially hypo-osmolar lumen condition affects the system. The first thing to notice is that for ratios of D_p/D_d which are greater than one (which is the most likely scenario for a gel or enema), the rate of change of volume of the body compartment actually changes signs at some point. This indicates that the osmolarity of the lumen compartment changed from hypo- to hyperosmolar relative to the body compartment. With D_p/D_d equal to 100, at around $t = 0.1$, the body compartment is back to its initial size and continues to shrink. This has significant repercussions on hypo-osmolar solutions used for drug delivery. In particular, the additional solutes used to form the delivery vehicle should be chosen such that their diffusivities are close to that of the drug in order to avoid the reversal of solvent flow which reduces the amount of drug that will reach its target. However, choosing a solute such that the ratio is smaller than one is unnecessary as the marginal benefits are negligible.

The same analysis performed on an initially hyperosmolar lumen condition is seen in Figure (3.8). The ratio of diffusivities still has a significant effect on the change in volume

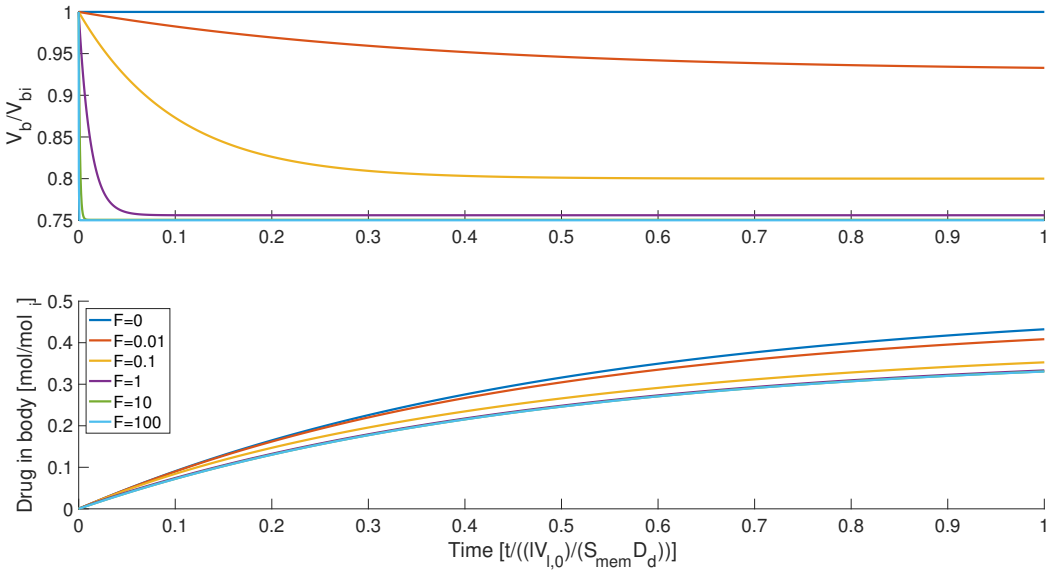

Figure 3.6: The top figure shows normalized body compartment volume as a function of time, and the bottom figure shows the normalized number of moles of drug that make it into the body compartment. The ratio of diffusivities of the drug and the passive solute is set equal to one, and ΔO is initially set to 0.2 (hyperosmolar lumen).

of the body compartment, but it ultimately has very little impact on the amount of drug delivered. This is an interesting result which implies that the choice of passive solute in a hyperosmolar solution is insignificant with respect to maximizing the amount of drug delivered.

3.4 Conclusions

In this chapter, we explored how osmolarity drives solvent flow across permeable membranes and can therefore be a strong influence on drug delivery. Osmolarity is the sum of concentrations of all species dissolved in a solvent. The drug-loaded solution will either be diluted or focused depending on the direction of solvent transport. If the drug is diluted because of a hyperosmolar initial lumen condition driving water out of the body, then the concentration difference is lowered which inhibits drug delivery. On the other hand, if the drug is focused in the lumen due to a hypo-osmolar initial lumen condition driving water into the body, then drug delivery behavior is enhanced.

A close scrutiny of the equations governing coupled solvent and solute transport led to the isolation of two nondimensional groups: 1) F, defined by the ratio of time scales of diffusive drug transport and initial solvent transport, and 2) D_p/D_d, the ratio of diffusivities of the passive solute and the drug. For a hypo-osmolar initial lumen case (possible for a gel

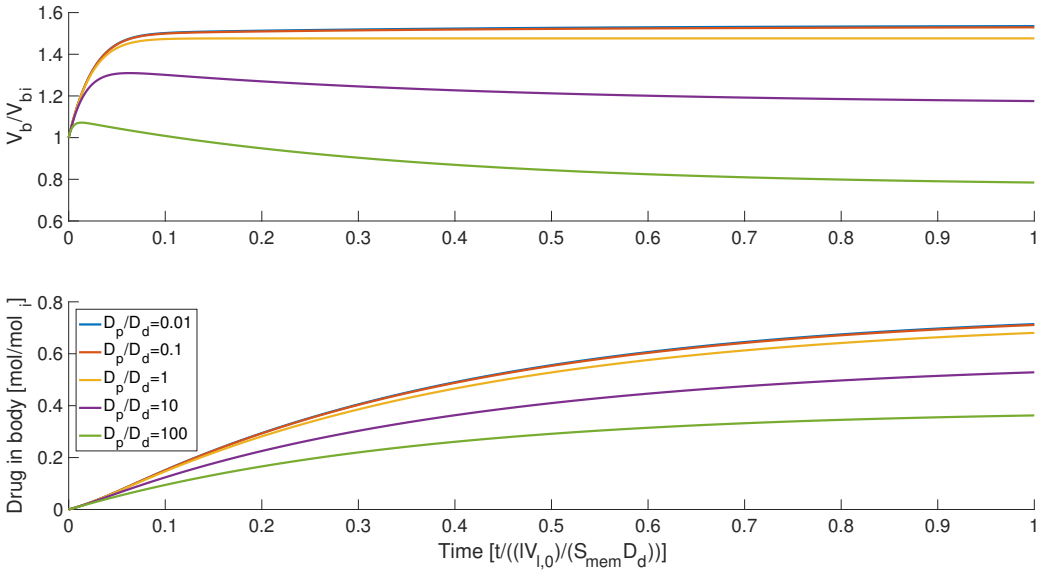

Figure 3.7: The top figure shows normalized body compartment volume as a function of time, and the bottom figure shows the normalized number of moles of drug that make it into the body compartment. The dimensionless group, F, is set equal to one, and ΔO is initially set to -0.2 (hypo-osmolar lumen).

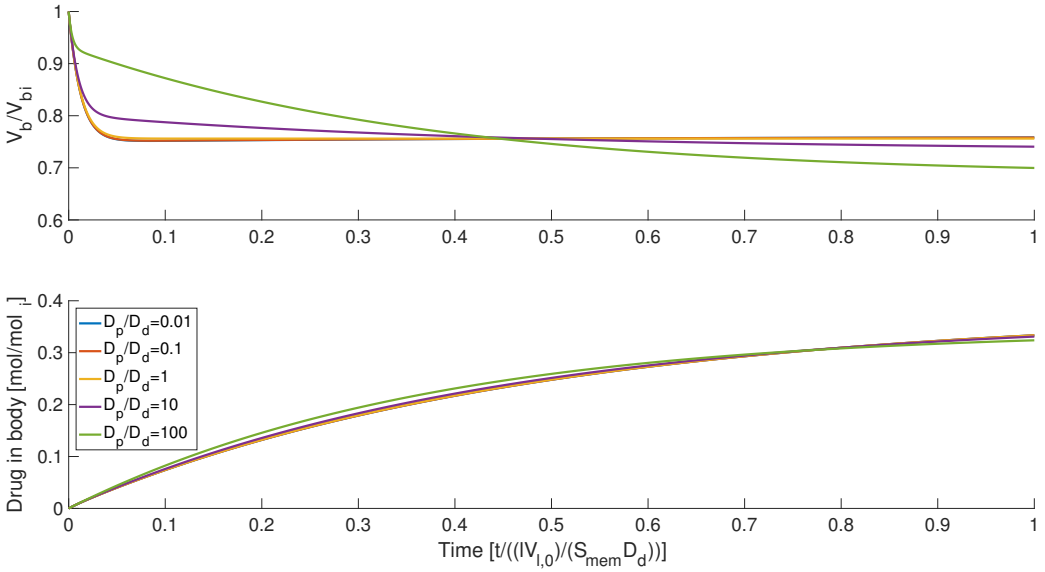

Figure 3.8: The top figure shows normalized body compartment volume as a function of time, and the bottom figure shows the normalized number of moles of drug that make it into the body compartment. The dimensionless group, F, is set equal to one, and ΔO is initially set to 0.2 (hyperosmolar lumen).

or enema), it is best to increase F if possible, but increasing F beyond one yields diminishing returns. It is also best for D_p/D_d to be greater than one for an initially hypo-osmolar initial lumen condition, though, again, increasing it beyond one sees no great benefit.

For a hyperosmolar initial lumen condition (as would likely be the case for a dissolving film, suppository, or pessary), decreasing F improves drug delivery characteristics to the limiting case of $F = 0$ which would be the case of zero solvent transport. The goal in this case is to limit the dilution of the drug concentration difference as much as possible to promote drug transport. Though influential on the rate of solvent transport, the ratio of D_p/D_d has little impact on the amount of drug delivered into the body compartment for an initially hyperosmolar initial lumen condition.

Chapter 4

Consequences of vaginal fluid production driven by osmolarity differences

In Chapter 2, vaginal anti-HIV drug delivery was simulated using a coupled model including gel spreading and diffusive drug transport. In order to include the effects of dilution, an average value of fluid production at the vaginal wall was assumed. In Chapter 3, osmolarity was investigated as a driver of fluid movement across permeable membranes. We showed that solvent flow can affect drug concentration gradients and therefore drug delivery. Here, we expand the usefulness of the model from Chapter 2 by incorporating concepts developed in Chapter 3.

4.1 Updating the model to include boundary dilution driven by osmolarity differences

The vaginal drug delivery model that we use has action occurring in three distinct compartments: the lumen into which the drug-loaded gel is inserted, the epithelium which is a thin protective layer of cells, and the stroma which is a muscular tissue perfused with capillaries. Similarly, in the osmolarity driven transport model there are three components which are analogous to the vaginal model: the lumen into which the drug is initially placed is the same, the permeable barrier representing the epithelium, and the body compartment into which the drug is transported representing the stroma.

The capillaries in skeletal muscle tissue like that of the stroma have pores with a maximum diameter of 5 nm [67]. The approximate diameter of a water molecule is 275 pm, and the approximate diameters of a sodium and chlorine ions are 454 pm and 350 pm respectively. Thus, water and dissolved NaCl will pass freely between the blood and the interstitial fluid. Blood is circulated through capillaries with a velocity of up to 1.5 $\frac{mm}{s}$, so we assume that

the osmolarity and concentration of sodium chloride in the extracellular fluid is replenished or washed out rapidly in order to maintain homeostasis at 300 mOsm within the stroma [65].

The permeability of vaginal epithelium is closely matched by that of non-keratinized buccal epithelium, so it is reasonable to use values of water permeability from buccal studies [8]. We therefore use a permeability value of $P = \frac{D_w}{l} = 450\frac{cm}{min}$ from Squier and Hall and follow their method of calculating diffusivity [72]. Permeability is defined as a diffusion constant divided by the permeable membrane's thickness which in this case is 20 μm. Thus, the effective diffusion constant of water through the epithelium is $1.5\text{x}10^{-6}\frac{m^2}{s}$. We assume that epithelial cells will maintain their volume without swelling or shrinking as water passes primarily through leaky junctions.

The universal placebo gel placed in the lumen is composed of water, hydroxyethylcellulose (HEC), NaCl, and sorbic acid [19]. Other gels may also contain glycerol or carbopol [29]. Glycerol, carbopol, and HEC are large molecules that will not easily be transported through the epithelium. We therefore assume that the total mass of these compounds remains constant in the lumen, and we assume that the local concentrations of these compounds will be proportional to the local gel fraction.The contribution of HEC to osmotic pressure is calculated as in Vink [83].

The osmolarity of the solution is controlled primarily through manipulation of the salt concentration in the gel as prepared, it is approximately iso-osmolar with the body in a standard universal placebo gel [19, 45, 86]. Recall that several conclusions were drawn concerning optimizing drug delivery based on manipulating a dimensionless group we called F. With a given drug, in this case Tenofovir, the only factor within F that we can manipulate is the initial difference in osmolarity which is controlled by the amount of salt used to prepare the gel. If we follow the suggestions made in Chapter 3, a hyperosmolar gel should be formulated to have the initial difference be as small as possible. If a hypo-osmolar gel is used, we suggested that the the gel be created such that F is greater than or equal to one, essentially lowering osmolarity to the greatest extent possible.

The diffusivity of solute through the cell membrane in the experiment performed by Knocikova et al. was approximately five orders of magnitude smaller than that of water, so salt will definitely move more slowly than water. For simplicity, we will assume here that salt is conserved in the lumen and will not pass through the epithelium over the time scale of interest in this study. The primary variable of interest is the transport of Tenofovir through the epithelium into the tissue which will almost certainly occur with more difficulty than that of salt. However, the overall contribution of salt transport to the water transport problem will likely be low due to small differences in concentration. We will therefore leave the inclusion of salt transport through the epithelium to future work. Again using the thinness assumption from Section 2.1, we assume that the conserved salt in the lumen will be well-mixed in the y-direction (on the time scale of interest) but may vary in the x-direction. The diffusivity of sodium ions through saline at body temperature is $12.01\text{x}10^{-6}\ \frac{cm^2}{s}$ according to Poisson and Papaud [60].

As a reminder, the dimensional set of equations describing solute and solvent flux as discussed in Chapter 3 are:

$$\frac{dV_l}{dt} = \frac{D_w MW_w S_{mem}}{l\rho_w}(O_l - O_b), \tag{4.1a}$$

$$\frac{dV_b}{dt} = -\frac{dV_l}{dt}, \tag{4.1b}$$

$$\frac{dc_{d,l}}{dt} = \frac{S_{mem}D_d}{l}\frac{c_{d,b} - c_{d,l}}{V_l} - \frac{c_{d,l}}{V_l}\frac{dV_l}{dt}, \tag{4.1c}$$

$$\frac{dc_{d,b}}{dt} = \frac{S_{mem}D_d}{l}\frac{c_{d,l} - c_{d,b}}{V_b} - \frac{c_{d,b}}{V_b}\frac{dV_b}{dt}, \tag{4.1d}$$

$$\frac{dc_{p,l}}{dt} = \frac{S_{mem}D_p}{l}\frac{c_{p,b} - c_{p,l}}{V_l} - \frac{c_{p,l}}{V_l}\frac{dV_l}{dt}, \tag{4.1e}$$

$$\frac{dc_{p,b}}{dt} = \frac{S_{mem}D_p}{l}\frac{c_{p,l} - c_{p,b}}{V_b} - \frac{c_{p,b}}{V_b}\frac{dV_b}{dt}, \tag{4.1f}$$

$$O_l = c_{d,l} + c_{p,l}, \tag{4.1g}$$

$$O_b = c_{d,b} + c_{p,b}. \tag{4.1h}$$

By assuming that the stroma maintains homeostasis with regards to fluid volume, we eliminate Equation (4.1b). In addition, the concentration of drug in the stroma is negligible in comparison to the concentration of salt (passive solute), so the homeostasis argument also allows us to eliminate Equation (4.1f). Drug transport is already taken care of in the gel simulation, so Equations (4.1c) and (4.1d) need not be solved here. In short, we have two equations to add to the gel model: one to track the change in fluid volume in the lumen, and one to track to change in passive solute (salt) concentration in the lumen. Keeping in mind that we will be neglecting the transport of salt across the epithelium, we neglect the first term on the right hand side of Eq (4.1e). We have assumed that osmolarity and fluid volume are constant in the stroma, and that the only solutes to cross the epithelium are the drug. We already have a drug concentration field integrated into the model, and we need to add an array of salt concentration in the lumen which is dependent on x-direction only.

In Section 2.1, we noted that the drug concentration is set to zero outside of the main volume of the bolus. Similarly, the initial lumen osmolarity is set to be iso-osmolar with the stroma outside of the main volume of the bolus. The concentration of salt ions is manipulated to achieve the desired osmolarities. For simplicity, in this calculation sodium and chloride ions are lumped together into a single salt ion concentration. Diffusion of salt through the lumen is solved using a simple forward time central space finite difference method. In order to remain stable, the maximum time step allowed by the adaptive scheme was reduced.

In the same section, we indicated that rheological behavior of the universal placebo gel was tested for gel fractions that ranged from 0.75 to 1.00. As a reminder, gel fraction (Φ) is the volume ratio of gel as prepared to gel as prepared plus extra diluting water. In the case of a hypo-osmolar initial lumen condition, the water is driven from the gel into the tissue such that the gel fraction will be driven to be greater than one assuming that there is no

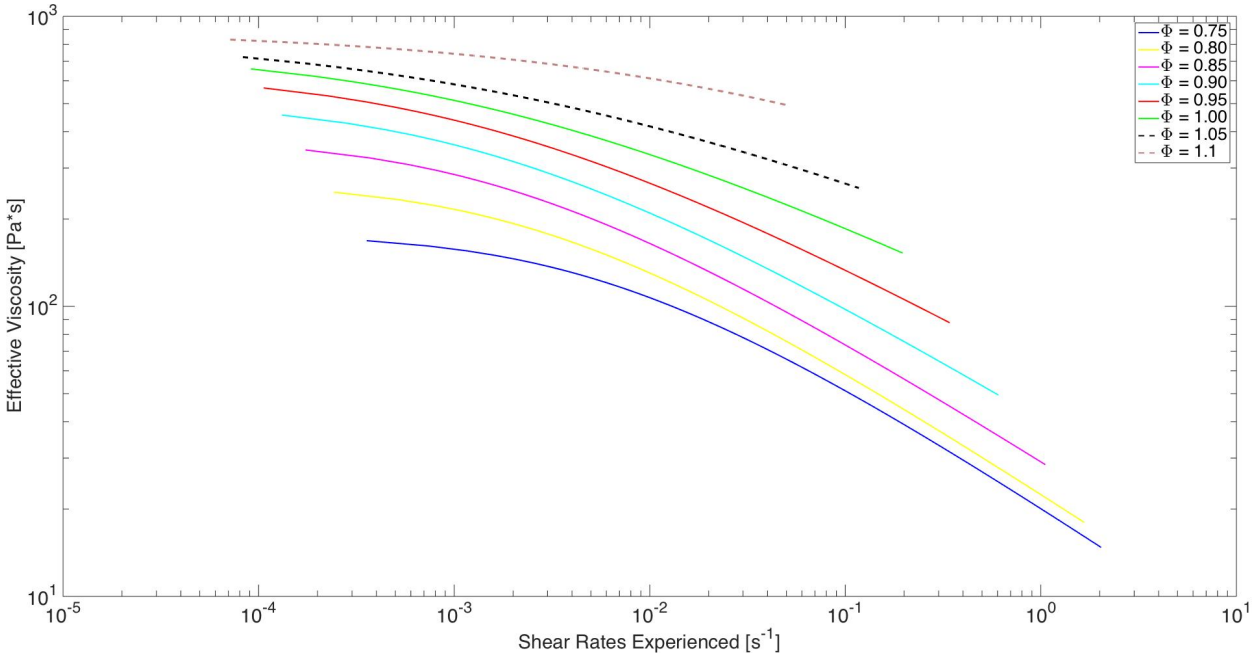

Figure 4.1: Curves of effective viscosity of the universal placebo as a function of shear rate and gel fraction. Note that the curves associated with Φ= [1.05,1.10] are extrapolated outside the available data.

initial dilution. The universal placebo gel is composed primarily of water, so this is not an unreasonable occurrence. Figure (4.1) shows the curves of effective viscosity of the universal placebo for a number of gel fractions. Although we are extrapolating the behavior of the gel outside of tested parameters, the similarity of the curves would suggest that this small extension is likely reasonable.

4.2 Results

The updated simulation was used to model five initial lumen osmolarities for the universal placebo gel: two hypo-osmolar solutions, an iso-osmolar solution, and two hyperosmolar solutions. The iso-osmolar solution was used as a control against previous simulations with zero flux in order to ensure that the system was behaving appropriately. Confirmation that wall flux and gel fraction remain unchanged within the limits of machine precision for an iso-osmolar solution is shown in Figure (4.2).

One of the key changes between this model and the one in Chapter 2 is that boundary flux is not a constant and can vary in both space and time. Figures (4.4a) and (4.3a) demonstrate this variation for a hypo-osmolar initial lumen condition (0.26 Osm) and hyperosmolar initial

lumen condition (0.34 Osm) respectively. The "shoulders" on either side of the main hump arise from the fact that the salt in the initial osmolarity condition diffuses slightly outside of the original bolus just like the initial concentration of the drug. This causes rapid dilution (or concentration) of the gel at the edges of the bolus which is ultimately smoothed out by the diffusion of salt and water through the gel.

We note that the order of magnitude of flux at early times is around $10^{-5}\frac{cm}{s}$ for a difference in osmolarity of ± 0.04 Osm as opposed to the constant flux previously used which was $-3.5\times10^{-7}\frac{cm}{s}$. (We note here that the generally accepted safety limit for a hyperosmolar gel is 1.2 Osm, a difference of 0.9 Osm, so we are well within these limits [19].) This difference in flux is quite large and means that a comparatively large amount of fluid is moving across the epithelium. However, integrated over the course of a four hour simulation, the total amount of fluid crossing the epithelium is less than half of what it would be using our constant boundary flux assumption.

Looking at profiles of gel fraction over time is another interesting exercise. Figures (4.4b) and (4.3b) demonstrate that the diffusion of water through the gel is fast enough eliminate the effects of the "shoulders" seen in the flux figures on the gel fraction and therefore on the rheological behavior of the gel. We also see that gel fraction normalizes more slowly than osmolarity. The flux becomes quite small within five minutes, but the gel fraction continues to become more uniform for nearly thirty minutes.

The reader will recall from the analysis done in Chapter 2 that we are interested in knowing the amount of drug that is delivered into tissue as well as the degree to which the gel spreads along the length of the vaginal canal. These values are intimately linked and allow us to extract information about the degree to which the rheological behavior of the gel influences the goal of drug delivery. All else held constant, increased spread length is directly correlated to an increase in the amount of drug that is delivered into tissue. However, increasing the spread length by diluting the gel also serves to dilute the drug concentration gradient which can result in decreased drug delivery. Hence, there is a trade-off.

We expect that as the hyperosmolar initial solutions will be diluted by boundary flux, their spread lengths will increase due to lowered viscosity. On the other hand, we expect the hypo-osmolar initial solutions to have a greater viscosity as water is driven into tissue which will lessen the degree to which the gel will spread. These expectations are confirmed in Figure (4.5b).

Although the initially hypo-osmolar solutions do not spread as far, they deliver more of the drug into the tissue than the hyperosmolar initial solutions and a comparable amount to the iso-osmolar initial solution as shown in Figure (4.5a). There is a competition between focusing the drug concentration in the lumen against reduced spreading from raised viscosities. The values are too close to one another to be distinguished in the figure, but it is interesting to note that increasing the degree of hypo-osmolarity increases the amount of drug delivered into tissue.

From what we had learned in our analysis of the effects of osmolarity on drug delivery in Chapter 3, we had expected that decreasing the initial osmolarity of the gel would improve drug delivery. This expectation was reinforced by the results shown by Xiao et al. and

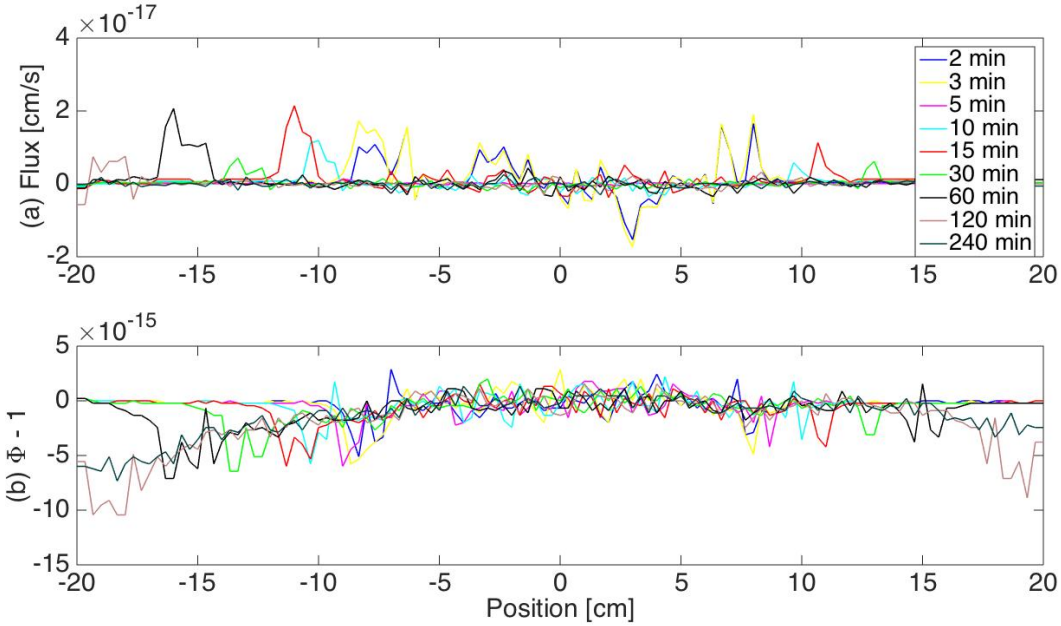

Figure 4.2: The flux of water into/ out of the lumen is zero to the order of machine precision in the case of an initially iso-osmolar solution seen in the top figure (a). Thus, it is not surprising that gel fraction only varies from its initial value within machine precision shown in figure (b).

Ensign et al. [86, 23]. Our results showing minimal changes in the amount of drug delivered into tissue were therefore initially rather surprising. The difference is accounted for by the rheological nature of the gel in use and the fact that it has to spread to allow the drug to transfer to tissue. Driving up the concentration gradient by forcing water into tissue was counteracted by the gel thickening and failing to spread sufficiently.

4.3 Engineering a Better Gel

Insights into the interplay of focusing the concentration gradient of the drug and thickening of the gel, both due to osmolarity driven solvent flux, suggest the possibility to engineer a better gel. We know that sufficient spreading at early times is critical to the ultimate amount

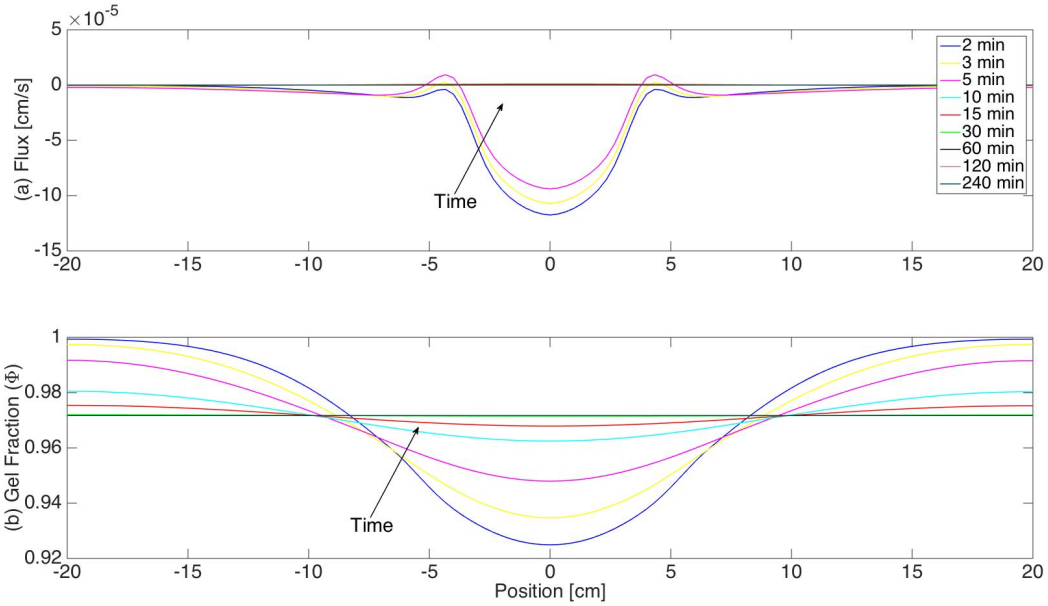

Figure 4.3: Water flux through the epithelium as a function of position is shown for various times in the upper figure (a). Negative flux values indicate that water is moving into the lumen from tissue. Gel fraction as a function of position is shown for various times in the lower figure (b). The initial osmolarity of the lumen is set to be hyperosmolar at a value of 0.340 Osm. Boundary flux diminishes more rapidly than gel fluid content equilibrates.

of drug delivered to tissue. Hyperosmolar gels promote early gel thinning and therefore spreading, but the decreased concentration gradient at the wall ultimately harms the goal of drug delivery. Hypo-osmolar gels increase the concentration gradient, but the decreased spreading due to gel thickening counteracts that benefit. Consider the possibility of a gel which is initially hyperosmolar, drawing fluid out of the tissue to promote early spreading, but over time converts to a hypo-osmolar solution via some sort of reaction which precipitates solutes out of solution perhaps as a consequence of changing pH or temperature. This gel would experience the benefits of both the increased early spreading of a hyperosmolar gel as well as the focused drug concentration of the hypo-osmolar gel.

Although the precise mechanism by which the osmolarity would be manipulated is unclear, the idea is conceptually sound as demonstrated by the work done by Nidhi et al. They developed a microbicidal gel with thermosensitive rheological characteristics and pH sensitive drug release characteristics [55]. Osmolarity is a property that is directly related to the chemical composition of the solution, so it is conceivable that there is a combination of solutes that would produce the desired precipitation response.

To test the possible effects, we ran the simulation again with an initially hyperosmolar gel and modeled precipitation with a reaction term proportional to the concentration of the salt in the gel. The reaction constant (10^{-5} s^{-1}) was chosen in order to see the effects

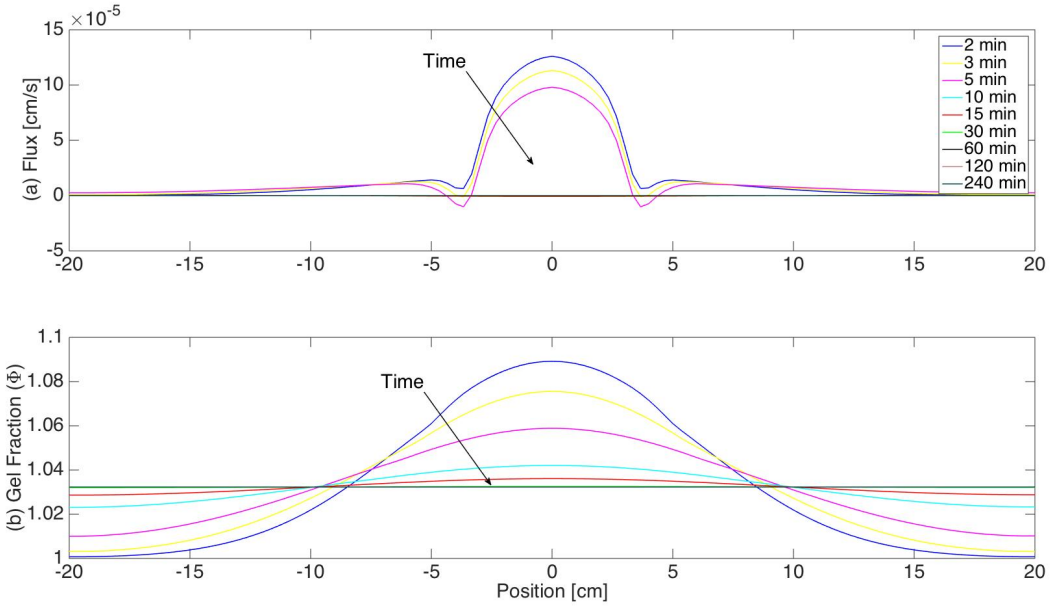

Figure 4.4: Water flux through the epithelium as a function of position is shown for various times in the upper figure (a). Positive flux values indicate that water is moving from the lumen into tissue. Gel fraction as a function of position is shown for various times in the lower figure (b).The initial osmolarity of the lumen is set to be hypo-osmolar at a value of 0.260 Osm. Boundary flux diminishes more rapidly than gel fluid content equilibrates.

of precipitation and maintain numerical stability. As anticipated, the spread length of the engineered gel (shown in Figure (4.6b)) initially tracks along the same trajectory as the corresponding hyperosmolar gel and then slows down as the osmolarity of the gel drops due to precipitation of the solutes. The boundary wall flux initially dilutes the gel, but the direction of fluid flow reverses between minutes five and ten (shown in Figure (4.7)).

4.4 Conclusions

This chapter combines concepts developed in the two previous chapters. The numerical model of gel spreading and drug diffusion developed in Chapter 2 was enhanced with the addition of osmolarity driven fluid flux developed in Chapter 3. Special attention was paid to the boundary conditions on the system of equations in order to simplify the calculations as much as possible while still retaining the effects of interest.

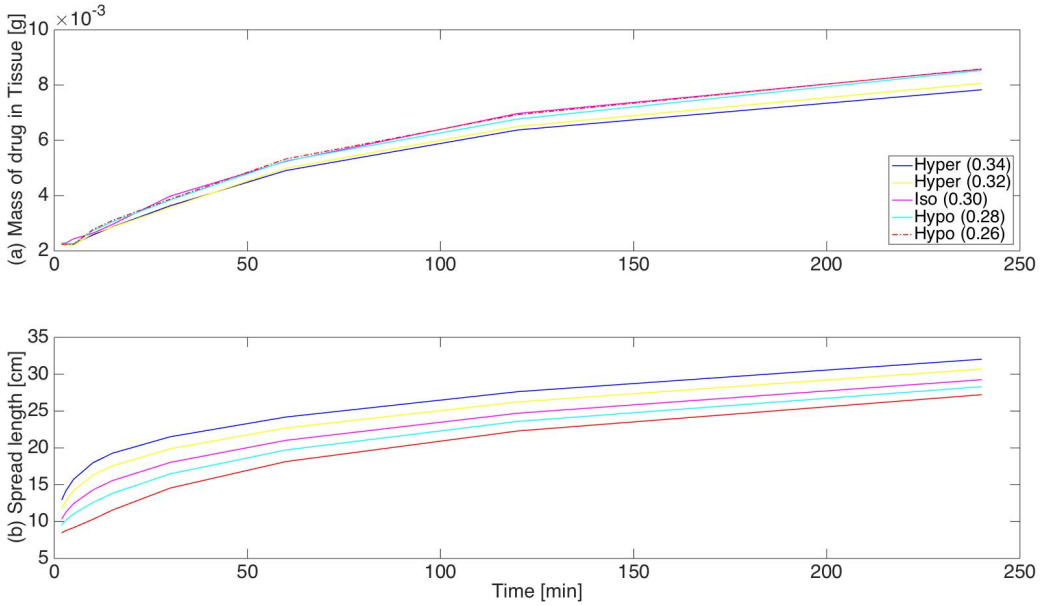

Figure 4.5: The amount of drug delivered into tissue as a function of time is shown in the top figure (a) for various initial lumen osmolarities. Their corresponding spread lengths are shown in the bottom figure (b). Spread length clearly increases with the initial osmolarity of the gel owing to boundary dilution. Long term drug delivery decreases with increasing initial osmolarity.

As expected, a hyperosmolar initial lumen condition resulted in decreased drug delivery due to drug concentration dilution from wall flux into the lumen. The dilution also resulted in increased spread lengths. Interestingly, a hypo-osmolar initial lumen condition did not result in increased drug delivery despite the focusing of the drug concentration in the lumen. The spread lengths of the hypo-osmolar gels were shortened due to gel thickening which negated the benefits of increasing the drug concentration gradient. The competing phenomena of gel thickening and drug focusing, both caused by the flow of water out of the lumen, suggest that decreasing osmolarity of gels without changing anything else about the gel would have limited effects on drug delivery.

A hypothetical engineered gel is proposed to harness the spreading benefits of a hyperosmolar solution as well as the drug focusing effects of a hypo-osmolar solution. A gel that is hyperosmolar at early times to promote early spreading but then becomes hypo-osmolar once spread in order to focus the drug in the lumen exhibits improved drug delivery results. Although we did not specify a mechanism to drive the solution from hyperosmolar to hypo-osmolar, the concept holds promise.

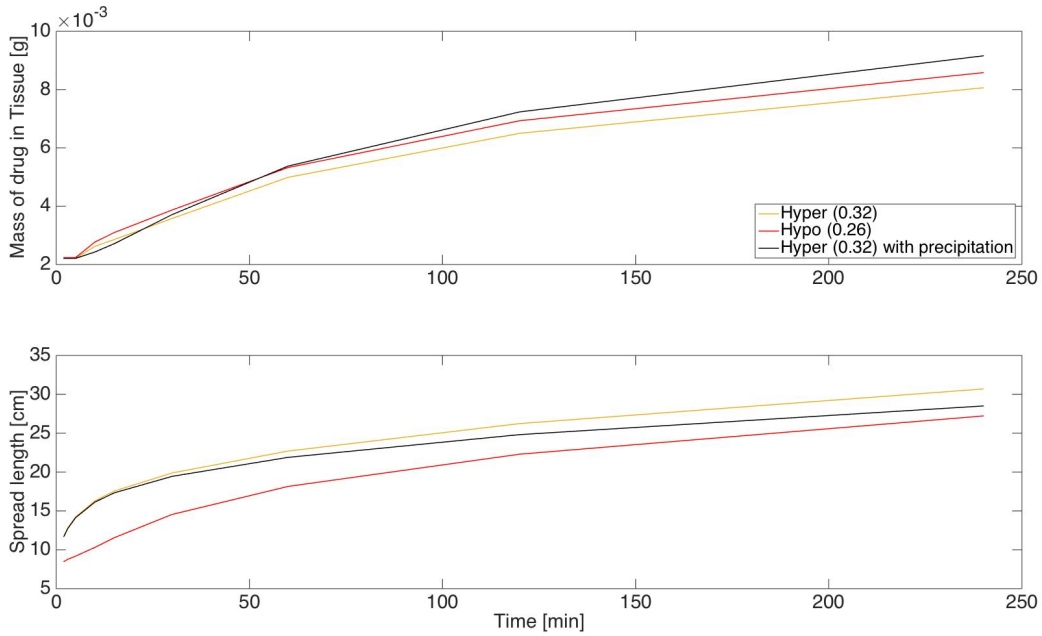

Figure 4.6: The amount of drug delivered into tissue as a function of time is shown in the top figure (a) for a hypo-osmolar gel, a hyperosmolar gel, and a hypothetical engineered gel. Their corresponding spread lengths are shown in the bottom figure (b). The engineered gel's spread length is in between that of the hyper- and hypo-osmolar gels, and its drug delivery performance is greater than that of the standard gels.

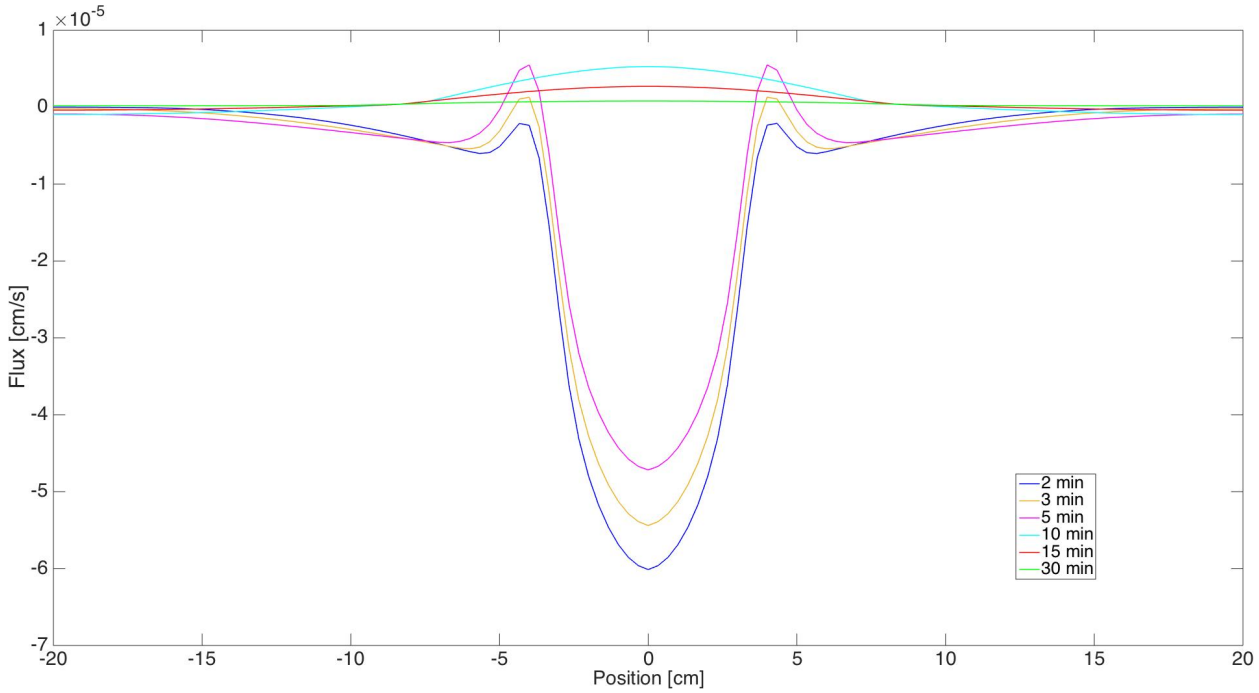

Figure 4.7: Water flux through the epithelium as a function of position is shown for various times for the hypothetical engineered gel. Negative flux values indicate water flow into the lumen, and positive values indicate water flow out of the lumen. When the engineered gel's osmolarity switches from hyperosmolar to hypo-osmolar relative to the body, the direction of flow changes.

Chapter 5

Recap

In Chapter 1, we demonstrated the need for ongoing research in the field of HIV prevention. Understanding the region in which the proposed intervention will be deployed as well as the ethical implications of performing research in economically disadvantaged regions is critical to the development of improved HIV prevention technologies. Current methods deployed in highly developed regions can be very effective, but the cost of such interventions can be prohibitive. HIV disproportionately affects women of sub-Saharan Africa where cultural and economic factors prevent the widespread use of oral PrEP and even discourage the use of condoms. This combination of circumstances suggests that microbicidal gel PrEP is a promising mode of preventing the spread of HIV in sub-Saharan Africa. As such, this is the field in which the remainder of the thesis focused.

In Chapter 2, we developed a numerical model of microbicidal gel spreading coupled with drug diffusion and tested it with three real gels and various levels of dilution. A thorough understanding of the differing time and length scales of the problem was necessary to do so in an efficient and accurate manner. The separation of time scales between gel spreading and drug diffusion allowed us to perform fewer costly finite element calculations which greatly decreased the computation time without losing precision. The separation of length scales within the lumen, among other things, allowed us to make the Reynolds lubrication approximation which greatly simplifies the equations used to solve for gel flow.

The rheological characteristics, specifically shear-thinning behavior and response to dilution, of the gels were of particular interest within the context of how they could influence the ultimate amount of drug which is delivered into tissue. We found that at early times when the shear forces on the gel are greatest, the rate of gel spreading is dominated by the shear-thinning of the gel which allows the bolus to spread faster. Early spreading is linked to increased drug delivery. Later spreading behavior is dominated by boundary dilution when the gel behaves primarily as a Newtonian fluid with progressively smaller viscosities. This progressive dilution reduces the concentration gradient between the lumen and the stroma which reduces the amount of drug that arrives into tissue.

It is interesting to note that the effects of boundary dilution on drug delivery are specific to the gel being studied. At early times, the boundary dilution aids the spreading process

which we know is tied to the amount of drug delivered into tissue. If the effects of boundary dilution on early spreading are stronger than its effects on diluting the concentration of the drug in the lumen, then boundary dilution can improve drug delivery behavior as is seen for IQB 3002. However, the effects are reversed for the universal placebo gel indicating that a thorough understanding of the rheological characteristics of the specific gel to be used are significant.

In Chapter 3, we chose to investigate osmolarity as a potential driver of boundary fluid dilution which we had previously assumed as a constant. Specifically, we explored how osmolarity drives solvent flow across permeable membranes and can therefore be a strong influence on drug delivery. Osmolarity is the sum of concentrations of all species dissolved in a solvent. The drug-loaded solution will either be diluted or focused depending on the direction of solvent transport. If the drug is diluted because of a hyperosmolar initial lumen condition driving water out of the body, then the concentration difference is lowered which inhibits drug delivery. On the other hand, if the drug is focused in the lumen due to a hypo-osmolar initial lumen condition driving water into the body, then drug delivery behavior is enhanced.

Close scrutiny of the governing equations yielded two nondimensional groups: 1) F, defined by the ratio of time scales of diffusive drug transport and initial solvent transport, and 2) D_p/D_d, the ratio of diffusivities of the passive solute and the drug. For a hypo-osmolar initial lumen case (possible for a gel or enema), it is best to increase F if possible, but increasing F beyond one yields diminishing returns. It is also best for D_p/D_d to be greater than one for an initially hypo-osmolar initial lumen condition, though, again, increasing it beyond one sees no great benefit.

For a hyperosmolar initial lumen condition (as would likely be the case for a dissolving film, suppository, or pessary), decreasing F improves drug delivery characteristics to the limiting case of $F = 0$ which would be the case of zero solvent transport. The goal in this case is to limit the dilution of the drug concentration difference as much as possible to promote drug transport. Though influential on the rate of solvent transport, the ratio of D_p/D_d has little impact on the amount of drug delivered into the body compartment for an initially hyperosmolar initial lumen condition.

Chapter 4 used the osmolarity driven solvent flow from Chapter 3 to enhance the numerical gel spreading and drug diffusion model from Chapter 2. Careful attention was paid to the boundary conditions on the system of equations in order to simplify the calculations as much as possible while still retaining the effects of interest.

As expected, a hyperosmolar initial lumen condition resulted in decreased drug delivery due to drug concentration dilution from wall flux. The dilution also resulted in increased spread lengths. Interestingly, a hypo-osmolar initial lumen condition did not result in increased drug delivery despite the focusing of the drug concentration in the lumen. The spread lengths of the hypo-osmolar gels were shortened due to gel thickening which negated the benefits of increasing the drug concentration gradient. The competing phenomena of gel thickening and drug focusing, both caused by the flow of water out of the lumen, suggest that decreasing osmolarity of gels without changing anything else about the gel would have

limited effects on drug delivery.

This suggested that an engineered gel could be proposed to harness the spreading benefits of a hyperosmolar solution as well as the drug focusing effects of a hypo-osmolar solution. A gel that is hyperosmolar at early times to promote early spreading but then becomes hypo-osmolar once spread in order to focus the drug in the lumen exhibits improved drug delivery results. Although we did not specify a mechanism to drive the solution from hyperosmolar to hypo-osmolar, the concept holds promise.

Ultimately, we state the contributions of this research as follows:

- We placed anti-HIV microbicidal gels into a cultural, economic, and ethical context.
- We developed a multi-scale, multi-step coupled model that incorporates gel spreading and drug diffusion in multiple interacting fluid-solid domains.
- We isolated the effects of rheological characteristics of the gels on drug delivery. Note that the effects may vary depending on the specific gel being studied.
- We isolated two nondimensional groups that determine the behavior of a drug delivery system that incorporates osmolarity driven fluid flow from the vaginal wall. Suggestions regarding the possible manipulation of these groups to enhance drug delivery were made.
- We incorporated osmolarity driven solvent flow into our gel spreading and drug diffusion model.
- We suggest the possibility of engineering a gel to harness the benefits of dilution based early spreading and drug concentration focusing by utilizing a precipitation type reaction.

Should this work be continued in the future, one proposed direction would be to verify experimentally the conclusions drawn concerning the effects of F and D_p/D_d on drug delivery. To do so, one would need to find several solutes for which their concentrations are easy to measure as well as a permeable membrane to place between two well-mixed baths. The dimensionless groups could then be tested independently with a variety of initial differences in osmolarity.

Additional experimental work could be done to determine model parameters that were assumed here. For example, the diffusivity of salt through the epithelium was assumed to be zero in Chapter 4, but that clearly is not the case. An experimental study would be useful in defining this parameter. We also assumed a crude model of a precipitation reaction, and further work is necessary to find the parameters of such a reaction.

It would also be worthwhile to develop a more sophisticated model for osmolarity driven flow within the larger numerical model. This could include modeling sodium and chlorine ions separately and potentially incorporating a non-constant boundary condition on these ions within the stroma. It would also be interesting to look at how the difference in pressure

(based on blood pressure) between the stroma and lumen may also be a contributing factor to the flow of solvent across the epithelium.

All of this work was done with the understanding that in order to design an effective drug delivery system, one must thoroughly understand the problem first. Computational models allow us to easily explore the physics of the problem and help us to uncover exciting and sometimes unexpected phenomena. Experimental work is vital to the advancement of the field, but it is much more useful when supplemented with computational simulations such as those performed here.

Bibliography

[1] Marcia Angell. "The Ethics of Clinical Research in the Third World". In: *The New England journal of Medicine* 337.12 (1997), pp. 847–849. ISSN: 0028-4793. DOI: 10.1056/NEJM199709183371209.

[2] Md Rajib Anwar, Kyle V. Camarda, and Sarah L. Kieweg. "Mathematical model of microbicidal flow dynamics and optimization of rheological properties for intra-vaginal drug delivery: Role of tissue mechanics and fluid rheology". In: *Journal of Biomechanics* 48.9 (2015), pp. 1625–1630. ISSN: 00219290. DOI: 10.1016/j.jbiomech.2015.01.049. URL: http://linkinghub.elsevier.com/retrieve/pii/S0021929015000652.

[3] Bertran Auvert et al. "Randomized, controlled intervention trial of male circumcision for reduction of HIV infection risk: The ANRS 1265 trial". In: *PLoS Medicine* 2.11 (2005), pp. 1112–1122. ISSN: 15491277. DOI: 10.1371/journal.pmed.0020298.

[4] Sarah J. Baird et al. "Effect of a cash transfer programme for schooling on prevalence of HIV and herpes simplex type 2 in Malawi: A cluster randomised trial". In: *The Lancet* 379.9823 (2012), pp. 1320–1329. ISSN: 1474547X. DOI: 10.1016/S0140-6736(11)61709-1. URL: http://dx.doi.org/10.1016/S0140-6736(11)61709-1.

[5] Kurt T Barnhart et al. "Baseline dimensions of the human vagina." In: *Human reproduction (Oxford, England)* 21.6 (2006), pp. 1618–22. ISSN: 0268-1161. DOI: 10.1093/humrep/del022. URL: http://www.ncbi.nlm.nih.gov/pubmed/16478763.

[6] F. Barre-Sinoussi et al. "Isolation of a T-Lymphotropic Retrovirus from a Patient at Risk for Acquired Immune Deficiency Syndrome (AIDS)". In: *Science* 220.4599 (1983), pp. 868–871.

[7] Chris Beyrer. "Pushback: the current wave of anti-homosexuality laws and impacts on health". In: *PLoS medicine* 11.6 (2014), e1001658. ISSN: 15491676. DOI: 10.1371/journal.pmed.1001658.

[8] P van der Bijl, I O Thompson, and C a Squier. "Comparative permeability of human vaginal and buccal mucosa to water." In: *European journal of oral sciences* 105.6 (1997), pp. 571–5. ISSN: 0909-8836. DOI: 10.1111/j.1600-0722.1997.tb00219.x. URL: http://www.ncbi.nlm.nih.gov/pubmed/9469607.

[9] B. Bingenheimer, Jeffrey. "Men's Multiple Sexual Partnerships in 15 Sub-Saharan African Countries: Sociodemographic Patterns and Implications". In: *Studies in Family Planning* 41.1 (2010), pp. 1–17. ISSN: 08966273. DOI: 10.1109/TMI.2012.2196707.Separate. arXiv: NIHMS150003.

[10] Alexander N. Brooks and Thomas J.R. Hughes. "Streamline upwind/Petrov-Galerkin formulations for convection dominated flows with particular emphasis on the incompressible Navier-Stokes equations". In: *Computer Methods in Applied Mechanics and Engineering* 32.1-3 (1982), pp. 199–259. ISSN: 00457825. DOI: 10.1016/0045-7825(82)90071-8.

[11] Lisanne Brown, Kate Macintyre, and Lea Trujillo. "Interventions to reduce HIV stigma: What have we learned?" In: *AIDS Education Prevention* 15.1 (2003), pp. 49–69. ISSN: 08999546. DOI: 10.1521/aeap.15.1.49.23844.

[12] CDC. *HIV and AIDS in America : A Snapshot*. 2016.

[13] M.S. Carvalho and L.E. Scriven. "Flows in Forward Deformable Roll Coating Gaps: Comparison between Spring and Plane-Strain Models of Roll Cover". In: *Journal of Computational Physics* 138.2 (1997), pp. 449–479. ISSN: 00219991. DOI: 10.1006/jcph.1997.5826. URL: http://linkinghub.elsevier.com/retrieve/pii/S0021999197958265.

[14] Centers for Disease Control and Prevention. "Current Trends Update: Acquired Immunodeficiency Syndrome (AIDS)–United States". In: *Morbidity and Mortality Weekly Report* 32.35 (1983), pp. 465–467. ISSN: 01492195. URL: http://www.cdc.gov/mmwr/preview/mmwrhtml/00000137.htm.

[15] Brian T. Chan and Alexander C. Tsai. "Trends in HIV-related Stigma in the General Population During the Era of Antiretroviral Treatment Expansion: An Analysis of 31 Sub-Saharan African Countries". In: *Journal of acquired immune deficiency syndrome* 72.2 (2016), pp. 558–564. DOI: 10.5588/ijtld.16.0716.Isoniazid.

[16] Oranat Chuchuen. "Development and Application of Raman Spectroscopy-Based Assays for Transport Analysis of Anti-HIV Microbicides in Gels and Tissues". PhD. Duke University, 2015. URL: http://hdl.handle.net/10161/11351.

[17] M. Cohen et al. "Prevention of HIV-1 Infection with Early Antiretroviral Therapy". In: *New England Journal of Medicine* 365.6 (2011), pp. 493–505. ISSN: 14783223. DOI: 10.1056/NEJMoa1105243.Prevention.

[18] Barry Coutinho and Ramakrishna Prasad. "Emtricitabine/tenofovir (Truvada) for HIV prophylaxis." In: *American family physician* 88.8 (2013), pp. 535–540. ISSN: 15320650.

[19] Ana Raquel Cunha et al. "Characterization of commercially available vaginal lubricants: A safety perspective". In: *Pharmaceutics* 6.3 (2014), pp. 530–542. ISSN: 19994923. DOI: 10.3390/pharmaceutics6030530.

[20] Maznah Dahlui et al. "HIV/AIDS related stigma and discrimination against PLWHA in Nigerian population". In: *PLoS ONE* 10.12 (2015), pp. 1–11. ISSN: 19326203. DOI: 10.1371/journal.pone.0143749.

[21] Damien De Walque et al. "Incentivising safe sex: A randomised trial of conditional cash transfers for HIV and sexually transmitted infection prevention in rural Tanzania". In: *BMJ Open* 2.1 (2012). ISSN: 20446055. DOI: 10.1136/bmjopen-2011-000747.

[22] Charles Dobard et al. "Postexposure protection of macaques from Vaginal SHIV infection by topical integrase inhibitors." In: *Science translational medicine* 6.227 (2014), 227ra35. ISSN: 1946-6242. DOI: 10.1126/scitranslmed.3007701. URL: http://www.ncbi.nlm.nih.gov/pubmed/24622515.

[23] Laura M. Ensign et al. "Enhanced vaginal drug delivery through the use of hypotonic formulations that induce fluid uptake". In: *Biomaterials* 34.28 (2013), pp. 6922–6929. ISSN: 01429612. DOI: 10.1016/j.biomaterials.2013.05.039. URL: http://dx.doi.org/10.1016/j.biomaterials.2013.05.039.

[24] FACTS. *HIV prevention study does not confirm tenofovir gel effectiveness Women require convenient and effective HIV prevention methods that work within the context of their lives*. 2015. URL: http://www.avac.org/sites/default/files/u3/FACTSfeb24.pdf.

[25] Nuno R Faria et al. "The early spread and epidemic ignition of HIV-1 in human populations". In: *Science* 346.6205 (2014), pp. 56–61. ISSN: 0036-8075. DOI: 10.1126/science.1256739.

[26] Adolph Fick. "On liquid diffusion". In: *The London, Edinburgh, and Dublin Philosophical Magazine and Journal of Science* 10.63 (1855), pp. 30–39. ISSN: 1941-5982. DOI: 10.1080/14786445508641925. URL: https://www.tandfonline.com/doi/full/10.1080/14786445508641925.

[27] Virginia A. Fonner et al. "Effectiveness and safety of oral HIV preexposure prophylaxis for all populations". In: *Aids* 30.12 (2016), pp. 1973–1983. ISSN: 14735571. DOI: 10.1097/QAD.0000000000001145.

[28] Henry Kaiser Family Foundation. *The Global HIV / AIDS Epidemic*. 2017.

[29] Claire Funke et al. "Coupled gel spreading and diffusive transport models describing microbicidal drug delivery". In: *Chemical Engineering Science* 152 (2016), pp. 12–20. ISSN: 00092509. DOI: 10.1016/j.ces.2016.05.015. URL: http://linkinghub.elsevier.com/retrieve/pii/S0009250916302548.

[30] Y. Gao et al. "Vaginal deployment and tenofovir delivery by microbicide gels". In: *Drug Delivery and Translational Research* 5.3 (2015), pp. 279–294. ISSN: 2190-393X. DOI: 10.1007/s13346-015-0227-1. URL: http://link.springer.com/10.1007/s13346-015-0227-1.

[31] Yajing Gao and David F Katz. "Multicompartmental pharmacokinetic model of tenofovir delivery by a vaginal gel." In: *PloS one* 8.9 (2013), e74404. ISSN: 1932-6203. DOI: 10.1371/journal.pone.0074404.

[32] M Thomas P Gilbert et al. "The emergence of HIV/AIDS in the Americas and beyond". In: *Proceedings of the National Academy of Sciences* 104.47 (2007), pp. 18566–18570. ISSN: 0027-8424. DOI: 10.1073/pnas.0705329104. URL: http://www.pnas.org/cgi/doi/10.1073/pnas.0705329104.

[33] Glenn Greenwald. *Drug Decriminalization in Portugal: Lessons for Creating Fair and Successful Drug Policies*. Washington D.C.: Cato Institute, 2009. DOI: 10.1126/science.246.4934.1104-a. URL: http://www.sciencemag.org/cgi/doi/10.1126/science.246.4934.1104-a.

[34] Geeta Rao Gupta et al. "Structural approaches to HIV prevention". In: *The Lancet* 372.9640 (2008), pp. 764–775. ISSN: 01406736. DOI: 10.1016/S0140-6736(08)60887-9.

[35] Anthony S Ham et al. "The rational design and development of a dual chamber vaginal / rectal microbicide gel formulation for HIV prevention". In: *ANTIVIRAL RESEARCH* 120 (2015), pp. 153–164. ISSN: 0166-3542. DOI: 10.1016/j.antiviral.2015.06.010. URL: http://dx.doi.org/10.1016/j.antiviral.2015.06.010.

[36] Catherine Hankins. "From a vicious circle to a virtuous circle: Reinforcing strategies of risk, vulnerability, and impact reduction for HIV prevention". In: *Lancet* 364.9449 (2004), pp. 1915–1916. ISSN: 01406736. DOI: 10.1016/S0140-6736(04)17488-6.

[37] Anke Hemmerling et al. "Lime Juice as a Candidate Microbicide? An Open-Label Safety Trial of 10% and 20% Lime Juice Used Vaginally". In: *Journal of Women's Health* 16.7 (2007), pp. 1041–1051. ISSN: 1540-9996. DOI: 10.1089/jwh.2006.0224. URL: http://www.liebertonline.com/doi/abs/10.1089/jwh.2006.0224.

[38] Kristen Hess et al. "Diagnoses of HIV Infection in the United States and Dependent Areas, 2016". In: *HIV Surveillance Report* 28 (2016). ISSN: 2169-575X. DOI: 10.1017/CBO9781107415324.004. arXiv: arXiv:1011.1669v3. URL: http://www.cdc.gov/hiv/library/reports/hiv-surveillance.html..

[39] David Holmes. "FDA paves the way for pre-exposure HIV prophylaxis". In: *The Lancet* 380.9839 (2012), p. 325. ISSN: 1474547X. DOI: 10.1016/S0140-6736(12)61235-5. URL: http://dx.doi.org/10.1016/S0140-6736(12)61235-5.

[40] John S. James. "Saquinavir (Invirase): first protease inhibitor approved–reimbursement, information hotline numbers". In: *AIDS Treat News* no 237 (1995), pp. 1–2. ISSN: 1052-4207.

[41] Quarraisha Abdool Karim et al. "Effectiveness and safety of tenofovir gel, an antiretroviral microbicide, for the prevention of HIV infection in women." In: *Science (New York, N.Y.)* 329.5996 (2010), pp. 1168–74. ISSN: 1095-9203. DOI: 10.1126/science.1193748.

[42] Ayesha B.M. Kharsany and Quarraisha A. Karim. "HIV Infection and AIDS in Sub-Saharan Africa: Current Status, Challenges and Opportunities". In: *The Open AIDS Journal* 10.1 (2016), pp. 34–48. ISSN: 1874-6136. DOI: 10.2174/1874613601610010034. URL: http://benthamopen.com/ABSTRACT/TOAIDJ-10-34.

[43] Sarah L Kieweg and David F Katz. "Interpreting properties of microbicide drug delivery gels: analyzing deployment kinetics due to squeezing." In: *Journal of pharmaceutical sciences* 96.4 (2007), pp. 835–50. ISSN: 0022-3549. DOI: 10.1002/jps.20774. URL: http://www.ncbi.nlm.nih.gov/pubmed/17094142.

[44] Sarah L Kieweg and David F Katz. "Squeezing flows of vaginal gel formulations relevant to microbicide drug delivery." In: *Journal of biomechanical engineering* 128.4 (2006), pp. 540–53. ISSN: 0148-0731. DOI: 10.1115/1.2206198. URL: http://www.ncbi.nlm.nih.gov/pubmed/16813445.

[45] Juliana A. Knocikova et al. "Mathematical Modeling of Cell Volume Alterations under Different Osmotic Conditions". In: *Biophysics and Medical Physics Computing Conference* 8.8 (2014), pp. 1164 –1168.

[46] Bonnie E. Lai et al. "Dilution of Microbicide Gels With Vaginal Fluid and Semen Simulants: Effect on Rheological Properties and Coating Flow". In: *Journal of pharmaceutical sciences* 97.2 (2007), pp. 1030–1038. ISSN: 1520-6017. DOI: DOI10.1002/jps.21132.

[47] Gilbert Newton Lewis. "The osmotic pressure of concentrated solutions, and the laws of the perfect solution". In: *Journal of the American Chemical Society* 30.5 (1908), pp. 668–683. ISSN: 15205126. DOI: 10.1021/ja01947a002.

[48] Kelsey MacMillan. "Coupled Pharmacodynamics from Transient Gel Spreading and Diffusive Transport into Tissue". Masters. University of California at Berkeley, 2014.

[49] Alamelu Mahalingam et al. "Vaginal microbicide gel for delivery of IQP-0528, a pyrimidinedione analog with a dual mechanism of action against HIV-1". In: *Antimicrobial Agents and Chemotherapy* 55.4 (2011), pp. 1650–1660. ISSN: 00664804. DOI: 10.1128/AAC.01368-10.

[50] Jean L Marx. "Strong New Candidate for AIDS Agent". In: *Science, New Series* 224.4648 (1984), pp. 475–477. ISSN: 0036-8075. DOI: 10.1126/science.6324344.

[51] Sheena McCormack et al. "PRO2000 vaginal gel for prevention of HIV-1 infection (Microbicides Development Programme 301): A phase 3, randomised, double-blind, parallel-group trial". In: *The Lancet* 376.9749 (2010), pp. 1329–1337. ISSN: 01406736. DOI: 10.1016/S0140-6736(10)61086-0. URL: http://dx.doi.org/10.1016/S0140-6736(10)61086-0.

[52] Microbicide Trial Network University of Pittsburgh and Magee-Womens Research Institute. *Study gel and applicator*. 2018. URL: http://www.mtnstopshiv.org/news/image-gallery (visited on 05/04/2018).

[53] Microbicide Trial Network. *MTN statement on decision to discontinue use of tenofovir gel in VOICE, a major HIV prevention study in women*. 2011. URL: http://www.mtnstopshiv.org/node/3909 (visited on 11/12/2014).

[54] Catherine M. Montgomery and Robert Pool. "Critically engaging: Integrating the social and the biomedical in international microbicides research". In: *Journal of the International AIDS Society* 14.SUPPL. 2 (2011). ISSN: 17582652. DOI: 10.1186/1758-2652-14-S2-S4.

[55] Kapadiya Nidhi et al. "Hydrotropy: A promising tool for solubility enhancement: A review". In: *International Journal of Drug Development and Research* 3.2 (2011), pp. 26–33. ISSN: 09759344. DOI: 10.1002/jps. arXiv: z0024.

[56] DH Owen, JJ Peters, and DF Katz. "Rheological properties of contraceptive gels". In: *Contraception* 62.2000 (2000), pp. 321–326. URL: http://www.sciencedirect.com/science/article/pii/S0010782400001840.

[57] Derek H. Owen and David F. Katz. "A vaginal fluid simulant". In: *Contraception* 59.2 (1999), pp. 91–95. ISSN: 00107824. DOI: 10.1016/S0010-7824(99)00010-4.

[58] Public Health Service (PHS). *Approval of AZT*. 1987. URL: https://aidsinfo.nih.gov/news/274/approval-of-azt.

[59] Audrey Pettifor et al. "Can money prevent the spread of HIV? A review of cash payments for HIV prevention". In: *AIDS and Behavior* 16.7 (2012), pp. 1729–1738. ISSN: 10907165. DOI: 10.1007/s10461-012-0240-z. arXiv: NIHMS150003.

[60] A. Poisson and A. Papaud. "Diffusion coefficients of major ions in seawater". In: *Marine Chemistry* 13.4 (1983), pp. 265–280. ISSN: 03044203. DOI: 10.1016/0304-4203(83)90002-6.

[61] Julie Pulerwitz and Gary Barker. "Measuring Attitudes toward Gender Norms among Young Men in Brazil". In: *Men and Masculinities* 10.3 (2008), pp. 322–338. ISSN: 1097-184X. DOI: 10.1177/1097184X06298778. URL: http://journals.sagepub.com/doi/10.1177/1097184X06298778.

[62] Thomas C. Quinn and Julie Overbaugh. "HIV/AIDS in Women: An Expanding Epidemic". In: *Science* 308.5728 (2005), pp. 1582–1583.

[63] Bill D Roberts. "HIV Antibody Testing Methods, 1985-1988". In: *Journal of Insurance Medicine* 26.1 (1994), pp. 13–14.

[64] S. Safren et al. "Adherence to Early Antiretroviral Therapy: Results from HPTN 052, A Phase III, Multinational Randomized Trial of ART to Prevent HIV-1 Sexual Transmission in Serodiscordant Couples". In: *Journal of acquired immune deficiency syndrome* 69.2 (2016), pp. 234–240. ISSN: 1527-5418. DOI: 10.1016/j.coviro.2015.09.001.Human. arXiv: 15334406.

[65] W Mark Saltzman. *Drug Delivery*. New York City: Oxford University Press, 2001, p. 368. ISBN: 9780471475736. DOI: 10.1002/0471475734.

[66] John S. Santelli, Ilene S. Spiezer, and Zoe R. Edelstein. "Abstinence Promotion Under PEPFAR: The Shifting Focus of HIV Prevention For Youth". In: *Global Public Health* 8.1 (2013), pp. 1–12. ISSN: 08966273. DOI: 10.1109/TMI.2012.2196707.Separate. arXiv: NIHMS150003.

[67] Hemant Sarin. "Physiologic upper limits of pore size of different blood capillary types and another perspective on the dual pore theory of microvascular permeability". In: *Journal of Angiogenesis Research* 2.1 (2010), pp. 1–19. ISSN: 20402384. DOI: 10.1186/2040-2384-2-14.

[68] Jill L. Schwartz et al. "A multi-compartment, single and multiple dose pharmacokinetic study of the vaginal candidate microbicide 1% tenofovir gel". In: *PLoS ONE* 6.10 (2011). ISSN: 19326203. DOI: 10.1371/journal.pone.0025974.

[69] Paul M. Sharp and Beatrice H. Hahn. "Origins of HIV and the AIDS pandemic". In: *Cold Spring Harbor Perspectives in Medicine* 1.1 (2011), pp. 1–22. ISSN: 21571422. DOI: 10.1101/cshperspect.a006841.

[70] Chyun Fung Shi, Michael Li, and Jonathan Dushoff. "Evidence that promotion of male circumcision did not lead to sexual risk compensation in prioritized Sub-Saharan countries". In: *PLoS ONE* 12.4 (2017), pp. 1–12. ISSN: 19326203. DOI: 10.1371/journal.pone.0175928.

[71] Drissa Sia et al. "What lies behind gender inequalities in HIV/AIDS in sub-Saharan African countries: Evidence from Kenya, Lesotho and Tanzania". In: *Health Policy and Planning* 29.7 (2014), pp. 938–949. ISSN: 14602237. DOI: 10.1093/heapol/czt075.

[72] C. A. Squier and B. K. Hall. "The permeability of skin and oral mucosa to water and horseradish peroxidase as related to the thickness of the permeability barrier". In: *Journal of Investigative Dermatology* 84.3 (1985), pp. 176–179. ISSN: 0022202X. DOI: 10.1111/1523-1747.ep12264711. URL: http://dx.doi.org/10.1111/1523-1747.ep12264711.

[73] Fred M. Ssewamala et al. "Effect of economic assets on sexual risk-taking intentions among orphaned adolescents in Uganda". In: *American Journal of Public Health* 100.3 (2010), pp. 483–488. ISSN: 00900036. DOI: 10.2105/AJPH.2008.158840.

[74] Ariane van der Straten et al. "Unraveling the divergent results of pre-exposure prophylaxis trials for HIV prevention." In: *AIDS (London, England)* 26.7 (2012), F13–9. ISSN: 1473-5571. DOI: 10.1097/QAD.0b013e3283522272. URL: http://www.ncbi.nlm.nih.gov/pubmed/22333749.

[75] Andrew J Szeri et al. "A model of transluminal flow of an anti-HIV microbicide vehicle: Combined elastic squeezing and gravitational sliding." In: *Physics of fluids* 20.8 (2008), p. 83101. ISSN: 1070-6631. DOI: 10.1063/1.2973188.

[76] S Tasoglu, DF Katz, and AJ Szeri. "Transient spreading and swelling behavior of a gel deploying an anti-HIV topical microbicide". In: *Journal of non-Newtonian fluid mechanics* (2012), pp. 36–42. DOI: 10.1016/j.jnnfm.2012.08.008.Transient.

[77] Savas Tasoglu et al. "The effects of inhomogeneous boundary dilution on the coating flow of an anti-HIV microbicide vehicle." In: *Physics of fluids (Woodbury, N.Y. : 1994)* 23.9 (2011), pp. 93101–931019. ISSN: 1070-6631. DOI: 10.1063/1.3633337.

[78] Savas Tasoglu et al. "Transient swelling, spreading, and drug delivery by a dissolved anti-HIV microbicide-bearing film." In: *Physics of fluids (Woodbury, N.Y. : 1994)* 25.3 (2013), p. 31901. ISSN: 1070-6631. DOI: 10.1063/1.4793598.

[79] T Turmen. "Gender and HIV/aids". In: *International Journal of Gynecology & Obstetrics* (2003). URL: http://www.sciencedirect.com/science/article/pii/S0020729203002029.

[80] UNAIDS. *UNAIDS Prevention Gap Report*. Tech. rep. 2016.

[81] U.S. Food and Drug Administration. *FDA approves first drug for reducing the risk of sexually acquired HIV infection*. 2012.

[82] Kristen Underhill. "Study designs for identifying risk compensation behavior among users of biomedical HIV prevention technologies: Balancing methodological rigor and research ethics". In: *Social Science Medicine* 94 (2013), pp. 115–123. ISSN: 15378276. DOI: 10.1080/10810730902873927.Testing. arXiv: NIHMS150003.

[83] H Vink. "Precision Measurements of Osmotic Pressure in Concentrated Polymer SOlutions". In: *European Polymer Journal* 7 (1971), pp. 1411–1419.

[84] Maretha J. Visser. "Life skills training as HIV/AIDS preventive strategy in secondary schools: Evaluation of a large-scale implementation process". In: *Sahara J* 2.1 (2005), pp. 203–216. ISSN: 18134424. DOI: 10.1080/17290376.2005.9724843.

[85] World Medical Association. "World Medical Association Declaration of Helsinki". In: *Bulletin of the world health organization.* 79.4 (2001), pp. 373–374. ISSN: 0042-9686. DOI: S0042-96862001000400016[pii]. URL: http://www.pubmedcentral.nih.gov/articlerender.fcgi?artid=2566407{\&}tool=pmcentrez{\&}rendertype=abstract.

[86] Peng Xiao et al. "Hypo-osmolar formulation of TFV enema promotes uptake and metabolism of TFV in tissues and leading to prevention of SHIV/SIV infection". In: *Antimicrobial Agents and Chemotherapy* October (2017). DOI: 10.1128/AAC.01644-17.